

The Pennsylvania State University
The Graduate School
Cell and Molecular Biology Program

**LIPOSOME-MEDIATED DOWN-REGULATION OF GASTRIN
IN PANCREATIC CANCER CELLS**

A Thesis in
Cell and Molecular Biology
by
Craig William Fenn

© 2009 Craig William Fenn

Submitted in Partial Fulfillment
of the Requirements
for the Degree of

Master of Science

May 2009

The thesis of Craig W. Fenn was reviewed and approved* by the following:

Jill P. Smith
Professor of Medicine
Thesis Adviser

Gail L. Matters
Assistant Professor of Biochemistry and Molecular Biology

Henry J. Donahue
Michael and Myrtle Baker Professor of Orthopaedics and Rehabilitation
Director of the Cell and Molecular Biology Graduate Program

*Signatures are on file in the Graduate School

ABSTRACT

Pancreatic cancer is among the most aggressive and lethal of all forms of cancer. Developing novel treatment strategies against pancreatic cancer can lead to increased survival time and increased chances for surgical removal of pancreatic tumors. Gastrin, a stomach hormone that is also produced by pancreatic cancer cells during the early stages of pancreatic cancer development, is a growth-stimulating factor that contributes to pancreatic cancer growth through binding to the cholecystokinin-2 receptor. Because of its growth-stimulating effects, gastrin is a potential target for therapeutic strategies. For that reason, lowering gastrin production could possibly also inhibit the growth of pancreatic cancer. To examine this possibility, we have developed a nanoliposome-based delivery system to deliver anti-gastrin siRNA to pancreatic cancer cells. These liposomes have been taken into various different pancreatic cancer cell lines *in vitro* and have also successfully encapsulated siRNA molecules targeting positions 90 and 286 of the gastrin mRNA. Liposome-encapsulated siRNAs have also been successfully transfected into the AsPC-1-Luc and BxPC-3-Luc cell lines, and have been able to down-regulate gastrin mRNA in both of these cell lines (determined via endpoint and quantitative real-time RT-PCR analysis). SiRNA targeted to position 286 of the gastrin mRNA has also down-regulated gastrin peptide via immunocytochemical analysis. SiRNA targeted to position 90 of the gastrin mRNA was then found to inhibit the growth of the BxPC-3-Luc cell line *in vitro* over a 10-day period. Finally, to determine the *in vivo* effectiveness of the liposome-mediated transfection system, liposome-encapsulated siRNAs against positions 90 and positions 286 of the gastrin mRNA were administered three times a week via

intravenous injection into athymic nude mice containing orthotopic BxPC-3-Luc tumors. The liposome/siRNA mixtures were not toxic to the mice, but did not provide significant down-regulation of gastrin mRNA and did not significantly decrease tumor size. However, the results obtained suggest a trend toward the down-regulation of gastrin mRNA as well as the inhibition of tumor growth. We conclude that while the liposome-mediated anti-gastrin siRNA delivery system we have developed has the potential for being an effective treatment strategy for pancreatic cancer, additional improvements to the system need to be made to increase transfection efficiency *in vitro* and *in vivo*.

TABLE OF CONTENTS

List of Figures.....	vii
List of Tables.....	ix
List of Abbreviations.....	x
Acknowledgements.....	xii
Chapter 1. Introduction.....	1
About Pancreatic Cancer.....	1
Gastrin.....	4
Small Interfering RNA.....	6
Liposomes.....	9
Summary of Research.....	11
Chapter 2. Materials and Methods.....	17
Cell Culture.....	17
Small Interfering RNA.....	17
Liposome Construction.....	18
Encapsulation of siRNA into Liposomes and Confirmation of Loading...	19
Determination of Liposome Encapsulation Capacity.....	20
<i>In Vitro</i> Transfection Methods (Oligofectamine and Liposomes).....	21
RNA Isolation from Cell Cultures.....	23
DNase I Treatment and Endpoint RT-PCR.....	23
Real-Time RT-PCR.....	25
Immunocytochemistry.....	27
<i>In Vitro</i> Growth Study.....	28
<i>In Vivo</i> Orthotopic Model of Pancreatic Cancer.....	29
Luciferase Imaging of Mouse Orthotopic Tumors.....	30
Randomization of Mice into Treatment Groups.....	31
Preparation of Liposomes and Injection of Liposomes into Mice.....	31
Sacrificing and Removal of Tissues From Mice.....	32
Analysis of Effects of Liposome Treatment on Orthotopic Tumors.....	33
Chapter 3. Results.....	40
100% and 75% pegylated liposomes have different siRNA loading capacities.....	40
Oligofectamine-mediated and liposome-mediated transfections of anti-gastrin siRNA down-regulate gastrin mRNA in AsPC-1-Luc cells...	41
Liposome-mediated transfection of anti-gastrin siRNA down-regulates gastrin mRNA in BxPC-3-Luc cells.....	42
Liposome-mediated transfection of anti-gastrin siRNA down-regulates	

gastrin peptide in BxPC-3-Luc cells.....	44
Liposome-mediated transfection of siRNA targeted to position 90 of the gastrin mRNA inhibits the growth of BxPC-3-Luc cells.....	44
Liposome-mediated siRNA treatment against orthotopic BxPC-3-Luc tumors in athymic nude mice does not significantly reduce gastrin mRNA or inhibit tumor growth.....	46
Chapter 4: Discussion of Results.....	68
Bibliography.....	74

LIST OF FIGURES

Figure 1-1: Histological and genetic changes in pancreatic cancer. From Ghaneh <i>et al.</i> (3).....	13
Figure 1-2: Signaling pathways induced by the CCK1 and CCK2 receptors. From Dufresne <i>et al.</i> (22).....	14
Figure 1-3: Sites of gastrin action in the stomach. From Dufresne <i>et al.</i> (22).....	15
Figure 1-4: The RNA interference pathway. From Gewirtz (60).....	16
Figure 2-1: Target sites on the gastrin mRNA of the siRNA molecules used.....	34
Figure 3-1: Electrophoresis showing 100% pegylated liposome loading capacity. Sterile 0.9% saline was the diluent for the liposomes.....	47
Figure 3-2: Electrophoresis showing 75% pegylated liposome loading capacity in sterile 0.9% saline (A) and dH ₂ O (B). Electrophoresis for both loading conditions was performed on the same gel.....	48
Figure 3-3: Endpoint RT-PCR for gastrin of RNA isolated from Oligofectamine- treated AsPC-1-Luc cells.....	49
Figure 3-4: Endpoint RT-PCR for GAPDH of RNA isolated from Oligofectamine-treated AsPC-1-Luc cells.....	50
Figure 3-5: Endpoint RT-PCR for gastrin of RNA isolated from liposome- treated AsPC-1-Luc cells, 1X liposome/siRNA formulation.....	51
Figure 3-6: Endpoint RT-PCR for GAPDH of RNA isolated from liposome- treated AsPC-1-Luc cells, 1X liposome/siRNA formulation.....	52
Figure 3-7: Endpoint RT-PCR for gastrin of RNA isolated from liposome- treated AsPC-1-Luc cells, 3X liposome/siRNA formulation.....	53
Figure 3-8: Endpoint RT-PCR for GAPDH of RNA isolated from liposome- treated AsPC-1-Luc cells, 3X liposome/siRNA formulation.....	54
Figure 3-9: Real-time RT-PCR for gastrin of RNA isolated from liposome- treated AsPC-1-Luc cells, 3X liposome/siRNA formulation and 300,000 cells per treatment. Graphs show relative quantity \pm the minimum and maximum relative quantities. Compared to the saline calibrator, SI 286 liposomes achieved down-regulation of gastrin mRNA at a P=0.0501 significance level	

by Student's T-test.....	55
Figure 3-10 : Endpoint RT-PCR for gastrin of RNA isolated from liposome-treated BxPC-3-Luc cells, 200,000 cells per treatment.....	56
Figure 3-11 : Endpoint RT-PCR for GAPDH of RNA isolated from liposome-treated BxPC-3-Luc cells, 200,000 cells per treatment.....	57
Figure 3-12 : Endpoint RT-PCR for gastrin of RNA isolated from liposome-treated BxPC-3-Luc cells, 125,000 cells per treatment.....	58
Figure 3-13 : Endpoint RT-PCR for GAPDH of RNA isolated from liposome-treated BxPC-3-Luc cells, 125,000 cells per treatment.....	59
Figure 3-14 : Real-time RT-PCR for gastrin of RNA isolated from liposome-treated BxPC-3-Luc cells, 200,000 cells per treatment. Graphs show average relative quantity \pm the maximum and minimum relative quantities (three replicates).....	60
Figure 3-15 : Real-time RT-PCR for gastrin of RNA isolated from liposome-treated BxPC-3-Luc cells, 125,000 cells per treatment. Graphs show average relative quantity \pm the maximum and minimum relative quantities (two replicates).....	61
Figure 3-16 : Immunocytochemical analysis of liposome/siRNA-treated BxPC-3-Luc cells.....	62
Figure 3-17 : Graph of growth inhibition by liposome-mediated transfection of siRNA targeted against position 90 of the gastrin mRNA in BxPC-3-Luc cells. Each data point indicates cell numbers \pm 1 standard deviation.....	63
Figure 3-18 : Tumor masses of liposome-treated orthotopic tumors in athymic nude mice. Graphs are tumor masses \pm 1 standard deviation.....	64
Figure 3-19 : Real-time RT-PCR for gastrin of RNA isolated from liposome-treated orthotopic BxPC-3-Luc tumors in athymic nude mice. Graphs are in fold expression of gastrin \pm the maximum and minimum relative quantities.....	65

LIST OF TABLES

Table 2-1: Nucleotide sequences of the siRNA molecules used.....	35
Table 2-2: Formulations for one in vitro liposome encapsulation of siRNA with control treatments (all volumes are in μL). Note: All volumes are scaled up for multiple treatments.....	36
Table 2-3: Formulations for liposome capacity test (all volumes are in μL).....	37
Table 2-4: Endpoint PCR primers for gastrin and GAPDH.....	38
Table 2-5: PCR cycles required for endpoint PCR of gastrin and GAPDH. The cycle numbers are variable due to differences between the cell lines.....	39
Table 3-1: Sedimentation of 100% pegylated liposome/siRNA mixtures prepared in sterile 0.9% saline.....	66
Table 3-2: Sedimentation of 75% pegylated liposome/siRNA mixtures prepared in 0.9% sterile saline and in dH_2O	67

LIST OF ABBREVIATIONS

The following abbreviations were used in this thesis:

PanIN: pancreatic intraepithelial neoplasia

IPMN: intraductal papillary mucinous neoplasm

MCN: mucinous cystic neoplasm

DNA: deoxyribonucleic acid

RNA: ribonucleic acid

siRNA: small interfering RNA

shRNA: short hairpin RNA

RNAi: RNA interference

GPCR: G protein-coupled receptor

CCK: cholecystokinin

CCK2R: cholecystokinin 2 receptor

MAPK: mitogen-activated protein kinase

ERK: Extracellular Signal-Regulated Kinase

ECL cell: enterochromaffin-like cell

HB-EGF: heparin-binding epidermal growth factor

RISC: RNA-induced silencing complex

PI3-kinase: Phosphoinositide 3-kinase

VEGF: vascular endothelial growth factor

PEG: polyethylene glycol

SNALP: stabilized nucleic-acid particles

BLAST: Basic Local Sequence Tool

mRNA: messenger RNA

mg: milligram

mL: milliliter

μ M: micromolar

μ L: microliter

μ g: microgram

dH₂O: distilled water

TAE: Tris-acetic acid-EDTA buffer

RNase: ribonuclease

DNase I: deoxyribonuclease I

PCR: polymerase chain reaction

RT-PCR: reverse transcription-polymerase chain reaction

GAPDH: glyceraldehyde 3-phosphate dehydrogenase

RT: reverse transcription

dNTPs: deoxyribonucleotides

cDNA: complimentary DNA

PPIA: peptidylprolyl isomerase A

EDTA: ethylenediaminetetraacetic acid

SPB: Sorenson's Phosphate Buffer

DPBS: Dulbecco's Phosphate Buffered Saline

ACKNOWLEDGEMENTS

The author would like to acknowledge the following: Dr. Jill Smith for serving as thesis mentor and providing technical and editorial advice; Dr. Gail Matters for providing technical and editorial advice, Dr. Mark Kester for his expertise with liposome construction; Christopher McGovern for his knowledge of laboratory methods, techniques, and statistical assistance; Calpurnia Jayakumar for her expertise in immunocytochemistry, fluorescent microscopy, and intravenous injection; The Penn State College of Medicine Functional Genomics Core Facility for quality control analysis of RNA samples and performing real-time PCR; Lionel Fonkoua for his efforts in the SURIP program during the Summer of 2008 and with the *in vivo* orthotopic studies in athymic nude mice; Kristin Fino and Krystal Anson for their assistance with the *in vivo* orthotopic studies in athymic nude mice; James Kaiser and Sriram Saravanan Shanmuga Velandy for their assistance in preparing liposomes; The Penn State Pathology Department for their pathological analysis of mouse tissues; The Penn State University College of Medicine Animal Research Facility for their care and maintenance of the athymic nude mice used in this study; and Dr. John Harms for the creation of many of the computer tools that were used to analyze data.

Chapter 1

Introduction

About Pancreatic Cancer

Pancreatic cancer, also known as pancreatic adenocarcinoma, is a cancer of the ductal epithelial cells of the pancreas. It is among the most aggressive and lethal forms of cancer. In the year 2008, it was estimated that in the United States 37,680 people will be diagnosed with pancreatic cancer, with an estimated 34,290 of those diagnosed dying. This is a 91% mortality rate (1). Even though relatively few people develop pancreatic cancer, its high mortality rate accounts for 6% of all of the cancer-related deaths in the United States. The overall five-year survival rate for pancreatic cancer is 5%. Pancreatic cancer is primarily a disease of older people; the majority of those diagnosed with pancreatic cancer are above 40 years of age and the median age of diagnosis is 73 years of age (1, 2).

The high mortality rate for pancreatic cancer is attributed to several factors. First, pancreatic cancer is often at an advanced stage when it is diagnosed, with the cancer having metastasized to organs such as the liver and the lungs. The five-year survival rate for locally invasive pancreatic cancer is less than 8%, and the five-year survival rate for pancreatic cancer that has metastasized to distant sites (such as the lungs) is only 2%. This is compared to a five-year survival rate of 20% if pancreatic cancer is diagnosed before metastasis occurs (1). Second, pancreatic cancer is also resistant to most common

chemotherapy agents, and those who qualify for surgical treatment, which is the most effective treatment option, only benefit from a small increase in survival time (3, 4).

There are several factors that increase the risk of developing pancreatic cancer. The first factor is age, as the majority of those who develop pancreatic cancer are above the age of 40. Second, smoking, which is the leading preventable risk factor, produces chemicals which are known to increase the risk of pancreatic cancer (2, 5, 6). Third, excessive alcohol consumption, like smoking, produces chemicals that are believed to contribute to increased risk (5). Fourth, dietary factors such as diets high in meats and fat, obesity, and diabetes mellitus increase the risk of developing pancreatic cancer (3). Fifth, hereditary predispositions to pancreatic cancer may be responsible for up to 10% of cases (2). Finally, pancreatitis, an inflammatory disease of the pancreas, generates scarring and increased cellular turnover, both of which are favorable conditions for the development of pancreatic cancer (2, 3).

Pancreatic cancer is a progressive disease, with cells developing and accumulating histological and genetic changes as they approach the cancerous stage. Histologically, the most common precursor lesions to pancreatic cancer are called pancreatic intraepithelial neoplasia (PanIN). PanIN lesions are divided into the following stages: PanIN-1A (the earliest), PanIN-1B, PanIN-2, and PanIN-3 (Figure 1-1)(3, 7, 8). Other, rarer precursor lesions that can also develop into pancreatic cancer but are not a part of this classification system are the Intraductal Papillary Mucinous Neoplasm (IPMN) and the Mucinous Cystic Neoplasm (MCN), both of which have histological characteristics different from PanIN lesions (3, 8, 9).

There are also many genetic abnormalities present in pancreatic cancer (Figure 1-1). The most significant mutation in pancreatic cancer is believed to be an activating mutation of the K-ras oncogene, which is found in up to 90% of all pancreatic cancer cases (4, 10). Also, the p53 tumor suppressor gene is mutated in up to 50% of pancreatic cancers (11). Other common mutations include: The p16/INK4A tumor suppressor gene, which is mutated in up to 95% of pancreatic cancers; the Smad4/transforming growth factor-beta pathway, which is mutated in up to 90% of pancreatic cancers (3, 12). Genes such as the HER2/NEU gene are overexpressed in pancreatic cancer, inducing increased cell division and growth (13). Also, signaling pathways originally active in fetal development, such as Notch and Hedgehog, are re-activated in pancreatic cancer and promote the development and invasiveness of pancreatic cancer (2, 3, 14). Collectively, these mutations contribute to increased cell growth and lowered restrictions on cell growth (3,4, 10, 11, 12, 13).

There are few treatment options for pancreatic cancer, and those treatment options that are available do not significantly increase the survival time for a person with pancreatic cancer. The most effective treatment option is the surgical removal of the tumor and surrounding tissues, which is called resection. However, this option is rare because the majority of pancreatic cancer cases are already at an advanced stage when diagnosed, and either do not qualify for surgery or surgery is not effective (2, 3, 15). Other treatment options include radiation therapy and chemotherapy, with the most common chemotherapy agent being the nucleotide analog Gemcitabine, which inhibits cancer growth by inhibiting DNA synthesis and inducing apoptosis (3, 16). However,

many other potential treatment targets may exist for pancreatic cancer, such as angiogenesis, matrix metalloproteinase, farnesyl transferase, and the epidermal growth factor (17, 18).

Gastrin

Gastrin is a peptide hormone of 17 amino acids in length, and is related to the hormone cholecystokinin (CCK). The human gastrin gene is located on chromosome 17 and contains three exons and two introns. The mRNA transcript is 434 base pairs in length which is processed and translated to yield the 17-amino acid product (19, 20, 21). Gastrin induces its effects through binding to its receptor, called the cholecystokinin-2 receptor (CCK2R) or “gastrin receptor” due to the fact that the receptor has high affinity for both gastrin and CCK, which also binds to the CCK2R via the same five amino-acid binding sequence (22, 23 24).

The CCK2R is a G protein-coupled receptor (GPCR) which induces its effects through many possible pathways (Figure 1-2) (22, 25, 26). The primary signaling cascade gastrin activates is the phospholipase C-beta signaling cascade, which can ultimately activate protein kinase D, the ERK family of MAP kinases, and nuclear factor κ -B (22, 27, 28). However, it can activate many other proteins, such as c-fos, c-Jun, and the JAK/STAT pathways (29, 30, 31).

Gastrin has many roles within the gastrointestinal tract. Its primary role is in the stimulation of acid secretion by the parietal cells of the stomach. It is secreted by the G cells of the stomach antrum and is produced in response to the stomach’s need for acid

production. Gastrin can stimulate acid secretion in two ways (Figure 1-3). The first way is by directly stimulating the parietal (acid-secreting) cells of the stomach to produce acid. The second is indirectly, by first stimulating the enterochromaffin-like (ECL) cells of the antrum to produce histamine, which then stimulates acid secretion by the parietal cells. Gastrin production is negatively regulated through the production of somatostatin by the D cells (22, 32, 33).

Gastrin is also a growth-promoting factor in the stomach, acting through the CCK2R and stimulating the growth and proliferation of gastric mucosal cells such as the ECL cells (34). This is accomplished by the transcriptional activation of genes such as the REG1 α gene, which increases the proliferative rate of the ECL cells and is also overexpressed in gastric cancers (22, 33). It is this growth-inducing effect which is important to gastric cancers (35), especially pancreatic cancer. Rat models have shown that gastrin is produced in the fetal pancreas, but is absent in adults (36). This is also the case for humans (37). Gastrin is believed to be overexpressed in pancreatic cancer cells beginning in the PanIN-2 stage of pancreatic cancer development (3), and has been found to induce growth-stimulating effects on pancreatic cancer cells, along with other gastric cancer cell lines (20, 28, 39). It is believed to be found in most patients with pancreatic cancer (40). It is believed to activate protein kinase B/Akt to induce the inactivation of the pro-apoptotic protein BAD in the rat pancreatic cancer cell line AR42J along with increasing the expression of the anti-apoptotic protein X-linked inhibitor of apoptosis in a gastro-esophageal cell line (33). Gastrin is also believed to induce angiogenesis through the transcriptional activation of heparin-binding epidermal growth factor (HB-EGF) (33,

41). In addition to HB-EGF, gastrin has also been found to increase the expression of other ligands of the epidermal growth factor receptor such as amphiregulin (33). In pancreatic cancer, gastrin is believed to act through an autocrine loop which may also involve the up-regulation of the CCK2R (42, 43, 44, 45, 77). In addition to the actions of the CCK2R, there is also evidence suggesting that a misspliced form of the CCK2R may also play a role in the increased proliferation of pancreatic cancer cells in a similar fashion (46, 47). This splice variant, called the “CCK-C receptor” by some, is believed to be present in 100% of pancreatic cancer cells and may also be constitutively active (48, 49). Watson and colleagues discovered that gastrin inhibition using antibodies can inhibit the growth rates of the pancreatic cancer cells lines PAN-1 and BxPC-3 when combined with the chemotherapeutic agents gemcitabine or taxotere (50), and developing treatment strategies targeting either gastrin or its receptor have been the subject of much research (50, 51, 52, 53, 54, 55, 56). For these reasons, gastrin targeting is an attractive choice for the inhibition of pancreatic cancer growth.

Small Interfering RNA

Small interfering RNA (siRNA) is a relatively new technology that is gaining popularity in biological research along with serving as a possible medical treatment strategy. The technology was first used successfully by Fire and Mello in the nematode *C. elegans*. They found that siRNA was much more effective at silencing gene expression than a related molecule called antisense RNA (57, 58). SiRNA has become a

popular way to examine gene expression and is also gaining interest as a possible treatment strategy for diseases such as cancer (59, 60).

Small interfering RNA molecules are double-stranded nucleotide sequences that can either be generated by synthetically or by cellular cleavage of larger double-stranded RNA molecules by the enzyme Dicer (Figure 1-4). Once siRNA is inside of the cell, whether by transfection or by cellular generation, it binds to the multi-protein complex called the RNA-induced silencing complex (RISC). The RISC degrades the sense strand of the double-stranded siRNA and uses the complimentary strand as a guide to scan messenger RNA molecules until the RISC-bound siRNA binds to a messenger RNA molecule (the “target” RNA) by complimentary base pairing. When this binding occurs, an enzyme present within the RISC then cleaves the target RNA, preventing the messenger RNA from being translated (60, 61, 62).

Small interfering RNA is related to two other gene silencing technologies: Antisense RNA and short hairpin RNA (shRNA). Antisense RNAs are single-stranded RNA molecules which bind to their complimentary RNA molecules by base pairing, preventing translation from occurring (61). Short hairpin RNAs, which are often introduced into cells via plasmid transfection, is processed by Dicer to generate siRNA molecules. The advantages that siRNA has over these other methods are: SiRNA takes advantage of the natural RNA interference pathway, siRNA is not required to bind to its target gene without assistance, it is only specific for the gene of interest, and it can potently block protein expression.

However, in order for siRNA to be an effective therapeutic tool against cancer

many challenges need to be addressed. Among those challenges are: The stability of the siRNA molecules in the bloodstream and serum (63, 64, 65), ensuring that the target cells receive the siRNA (63), proper design and bioinformatic analysis to ensure that the siRNA has no off-target gene silencing effects (66, 62), avoiding the 5' and 3' untranslated regions of the target mRNA, having a GC content of around 50% (62), a nucleotide length of between 21 and 23 nucleotides (62), avoiding possible oversaturation problems that have been observed with short hairpin RNAs (67), and developing an effective delivery system for the siRNA so that the siRNA can avoid destruction by serum endonucleases and exonucleases as well as removal by the excretory system (58, 61, 68, 69).

SiRNA technology may be a potential therapeutic strategy for pancreatic cancer and other gastrointestinal cancers. RNA interference has been accomplished in non-human primates against the ApoB gene using a lipid-based delivery system (70). Potential siRNA therapeutic targets include PI3-kinase and cyclooxygenase-2 in colon cancer, the anti-apoptotic protein BCL-X_L in esophageal cancer (71), and the vascular endothelial growth factor gene in pancreatic cancer, which Wang and colleagues were able to down-regulate in BxPC-3 pancreatic cancer cells, inhibiting their growth (72).

With regards to gastrin and pancreatic cancer, gene silencing via siRNA may be a promising strategy to slowing the progress of this quickly-moving disease. Smith and colleagues used antisense RNA against gastrin to down-regulate gastrin and inhibit growth in the BxPC-3 pancreatic cancer cell line (73). Watson and colleagues, using an amine-based and a lipid-based transfection reagent, employed siRNAs targeted against

various sites of the gastrin gene. They used these anti-gastrin siRNAs to lower gastrin gene expression in the PAN-1 pancreatic cancer cell line, with the most significant lowering obtained with siRNA molecules targeted to positions 248 and 251 of the gastrin messenger RNA (19). Given this previous record of inhibiting gastrin gene expression to inhibit pancreatic cancer cell growth, it is conceivable that an siRNA-based treatment could be developed for the treatment of pancreatic cancer.

Liposomes

In order for siRNA to be a treatment strategy, an effective delivery method needs to exist. There are many possible delivery systems for siRNA, and each system has strengths and weaknesses. Among those methods attempted *in vivo* are: Injection of naked siRNA into the bloodstream, local administration of siRNA to the tissue of interest, conjugating the siRNA to cholesterol, chemically modifying the siRNA molecule, and polymer-based carrier methods (58, 61, 68). The delivery method we have chosen for the delivery of anti-gastrin siRNA molecules is the liposome. Liposomes are small (between 40 nm and 100 nm in diameter) lipid vesicles which can carry small molecules such as drugs to cells. The liposomes are generated by first chemically combining the lipids, which is then followed by a process called extrusion. During extrusion, lipid mixtures are moved under high pressure through a polycarbonate filter system of a specific size, only allowing particles of the size of the filter to pass through. The liposomes are then stored in the appropriate solvent (usually saline solution) until they are used (74, 75, 76).

To encapsulate negatively-charged nucleic acid molecules, liposomes need to be cationic (carry a positive charge) to allow the nucleic acids to be attracted to the lipids. Also, liposomes must contain lipids conjugated to polyethylene glycol (PEG) to stabilize the liposome structure and protect liposomes from destruction *in vivo* (74, 78, 80). The encapsulation of siRNA generates liposomal nanoparticles of neutral charge called stabilized nucleic-acid particles (SNALPs) which have the siRNA molecules inside of the lipid covering. The presence of successfully encapsulated siRNA within SNALPs can be resolved by electrophoresis (74, 76). The liposome delivers its contents to the cell by first fusing to the cell membrane and then the contents enter the cell by endocytosis (79).

What makes liposome technology so powerful is its versatility. Liposomes are able to carry small molecule drugs, chemotherapeutic agents, and nucleic acids (74, 80, 81). They can carry a neutral charge, positive charge (cationic), or a negative charge (anionic). The lipid molecules can be modified to attach to peripheral molecules such as antibodies and peptides. For example, Pastorino and colleagues attached a peptide called the NGR peptide to liposomes via a maleimide linkage, allowing the liposomes to be specifically targeted to angiogenic endothelial cells and deliver the drug doxorubicin to the endothelial cells (82). Second, cationic and anionic liposomes have been constructed to target cells that express the folate receptor (83, 84), and liposomes have been developed to target the alpha-1 integrin in endothelial and melanoma cells (85). Finally, liposomes targeted to the beta-1 integrin that contain protamine-compacted siRNA against the messenger RNA for cyclin D1 silenced cyclin D1 expression in mice, and was called a “technical tour de force” by Science magazine (86).

However, the use of liposomes as effective drug carriers has some challenges. Among those challenges include: Toxicity in the the body (87), circulation in the bloodstream for prolonged periods of time, recognition by the immune system, clearance by the reticuloendothelial system, clearance by the kidneys (80, 88, 89), delivery method into the body (81), the size of the liposomes, and the charge of the liposomes (90). The presence of polyethylene glycol groups on liposomes protect liposomes from attack by the immune system via opsonization (80), increase circulation time in the bloodstream, and increase uptake efficiency of the drug carried in the liposomes (78), making pegylated liposomes promising tools for drug delivery for tumors (91). Other modifications can also maximize liposome transport effectiveness and limit toxicity (87). For example, liposomes targeting transferrin-receptor-containing cells have been developed and can carry siRNA without toxic effects in non-human primates (92).

Summary of Research

We have begun to develop a liposome-mediated delivery system for delivering anti-gastrin siRNA to pancreatic cancer cells. The specific lipids and the pegylation ratios have been optimized for siRNA delivery into the AsPC-1-Luc and BxPC-3-Luc pancreatic cancer cell lines. This delivery system down-regulated gastrin mRNA in both cell lines, as well as gastrin peptide in the BxPC-3-Luc cell line. This delivery method has also inhibited the growth of pancreatic cancer cells *in vitro* and *in vivo*. However, the lack of consistent statistical significance of gastrin mRNA down-regulation suggests that additional improvements need to be made to optimize the effects of the liposome-

mediated anti-gastrin siRNA delivery system *in vitro* and *in vivo*.

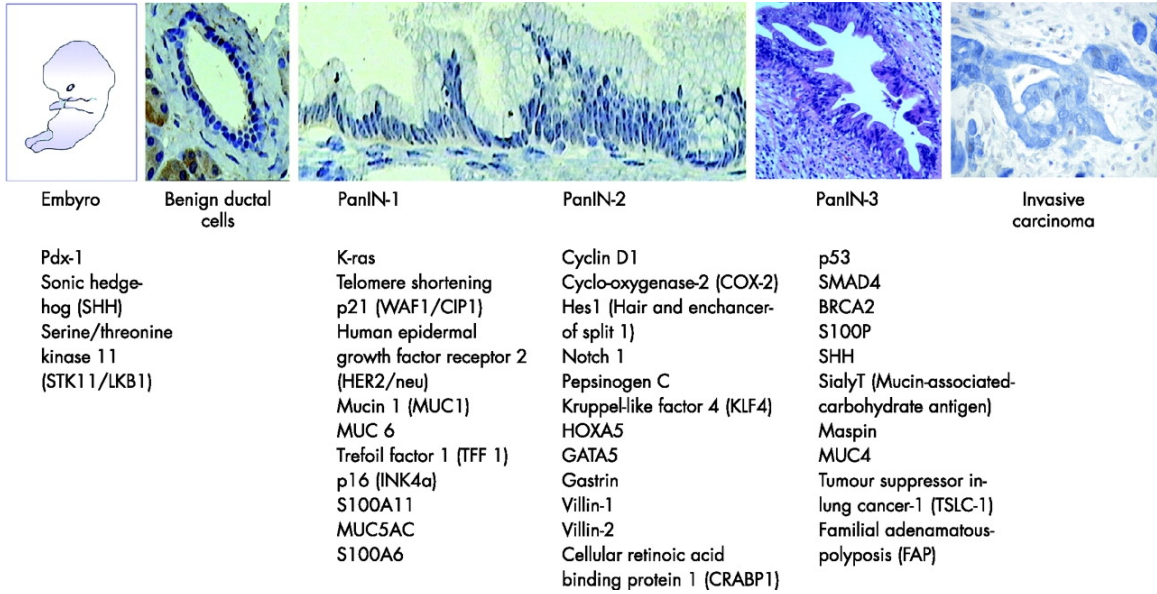


Figure 1-1: Histological and genetic changes in pancreatic cancer. From Ghaneh *et al.* (3)

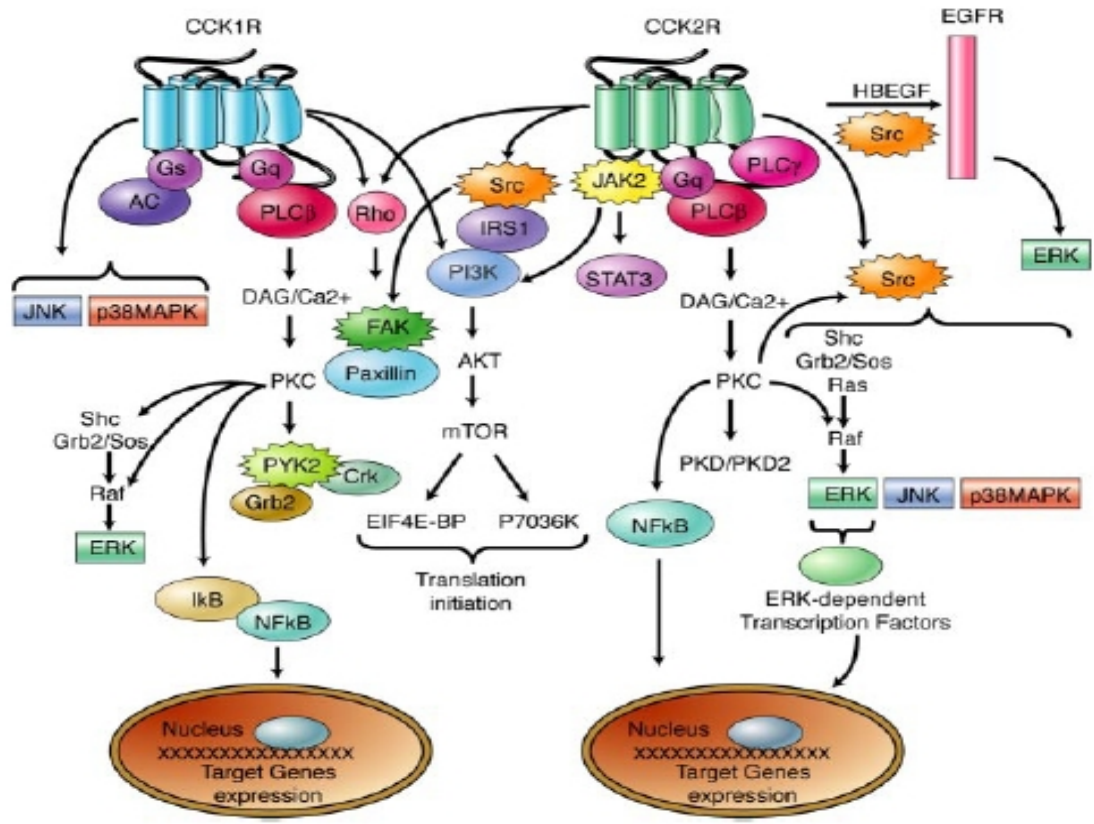


Figure 1-2: Signaling pathways induced by the CCK1 and CCK2 receptors. From Dufresne *et al.* (22).

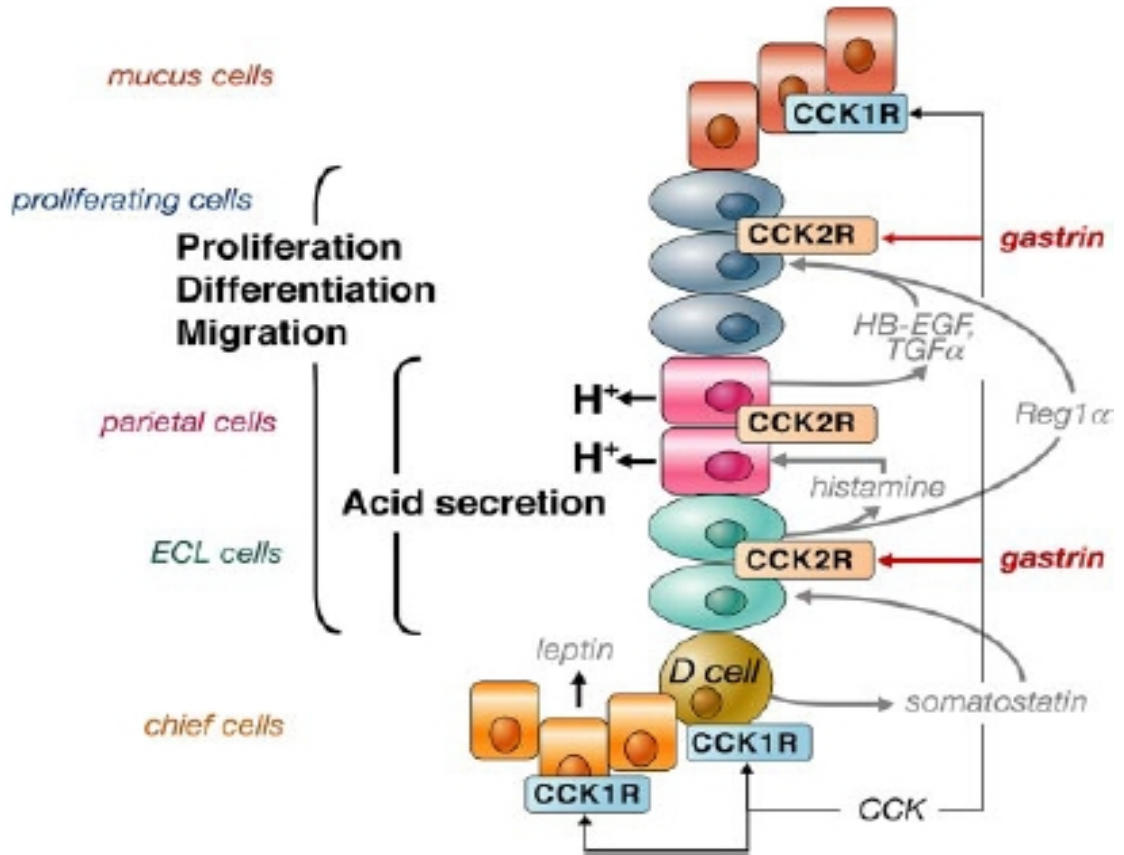


Figure 1-3: Sites of gastrin action in the stomach. From Dufresne *et al.* (22).

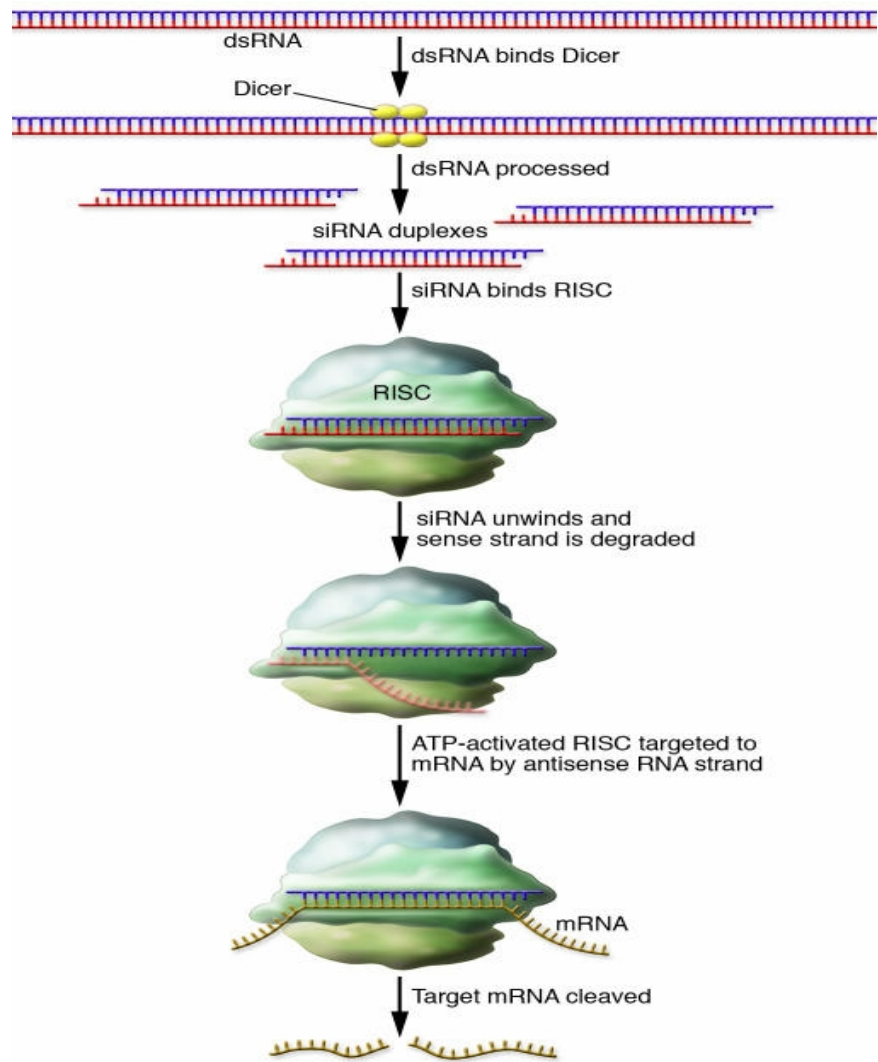


Figure 1-4: The RNA interference pathway. From Gewirtz (60).

Chapter 2

Materials and Methods

Cell Culture

ASPC-1-Luc and BxPC-3-Luc cells were obtained from the laboratory of Craig Logsdon (University of Texas M.D. Anderson Cancer Center). The cells were maintained in RPMI 1640 medium containing 10% fetal calf serum in an incubator kept at 37°C and 5% CO₂. Both of the cell lines are derived from pancreatic adenocarcinoma (93), express the CCK2 receptor (94), and express a luciferase reporter gene which allows to image the cells *in vivo*.

Small Interfering RNA

Anti-gastrin small interfering RNA molecules have been developed to target positions 90 and 286 of the gastrin mRNA (Figure 2-1, Table 2-1). The sequences of the siRNAs and scrambled control siRNAs used were developed with technical assistance from OligoEngine, who used the BLAST (Basic Local Sequence Tool) to determine and minimize potential off-target effects of the siRNAs. SiRNA molecules were purchased from both OligoEngine (for earlier studies using AsPC-1-Luc cells) and from Invitrogen (for later *in vitro* studies using AsPC-1-Luc cells and for *in vitro* and *in vivo* studies using BxPC-3-Luc cells). Only the siRNA targeted against position 286 of the gastrin mRNA was used to treat AsPC-1-Luc cells, while siRNA targeted against both positions 90 and

286 were used to treat BxPC-3-Luc cells *in vitro* and *in vivo*. Upon receipt of the lyophilized siRNAs, RNase-free water (Qiagen) was added to hydrate the siRNA and set the stock concentration to 100 μ M. The siRNA stock solutions were distributed into 20 μ L aliquots which were then diluted with RNase-free water to a working concentration of 20 μ M.

Liposome Construction

Cationic nanoliposomes of 70 nm diameter were synthesized in the laboratory of Mark Kester (Pennsylvania State University College of Medicine, Department of Pharmacology) by James Kaiser and Sriram Saravanan Shanmuga Velandy. Liposomes containing 100% pegylation were synthesized by the method described in Tran et al. (76). Briefly, the liposomes were synthesized by combining 1,2-Dioleoyl-3-Trimethylammonium-Propane Chloride (DOTAP), 1,2-Dioleoyl-sn-Glycero-3-Phosphoethanolamine (DOPE), and 1,2-distearoyl-sn-glycero-3-phosphoethanolamine-N-[methoxy(polyethylene glycol)-2000] (DSPE-PEG 2000) (Avanti Polar Labs) in chloroform at a 4.75: 4.75: 0.5 molar ratio. Liposomes containing 75% pegylation were also generated with 75% of the volume of the DSPE-PEG 2000 used in the formulation described above. All liposome solutions were stored in isotonic saline solution at a concentration of 25 mg liposomes per mL of solution. The 100% pegylated liposomes were used on AsPC-1-Luc cells and the 75% pegylated liposomes were used on BxPC-3-Luc cells. The different pegylation percentages were based on an uptake experiment done in our laboratory using unlabeled and rhodamine-labeled liposomes of 100% and

75% pegylations that established which liposomes were appropriate for treatment of both cell lines (Smith J, unpublished data).

Encapsulation of siRNA into Liposomes and Confirmation of Loading

For *in vitro* and *in vivo* liposome treatments, Table 2-2 shows the volumes for a typical liposome encapsulation of siRNA used for *in vitro* and *in vivo* liposome treatments (also called a “1X” liposome treatment). All liposome encapsulations were performed in sterile conditions in a laminar flow hood. All solutions were mixed in microcentrifuge tubes in the following order: (1) 0.9% sterile saline, (2) 20 μ M siRNA, and (3) 25 mg/mL empty liposomes. The liposomes were added in a dropwise fashion, and the tubes were tapped to ensure thorough mixing. The resulting liposome/siRNA mixtures were then left overnight at room temperature to ensure complete encapsulation.

To confirm liposome encapsulation of siRNA, the tubes containing the liposome/siRNA mixtures were first visually inspected by holding them up to light. Any particulate matter (called “sedimentation”) in the tubes suggests “crashing out” of the liposomes, meaning that the liposomes were unable to hold the siRNA. “Crashing out” eliminates the transfection ability of the liposome/siRNA complex.

In addition to visual inspection of the liposome/siRNA mixtures, encapsulation was also confirmed by agarose electrophoresis. 10 μ L of each liposome preparation was mixed with 10 μ L of ghost loading buffer (30% glycerol in dH₂O). As a size control, 10 μ L of 20 μ M siRNA was mixed with 10 μ L of ghost loading buffer. 10 μ L of each resulting mixture was loaded into a 2% agarose gel containing ethidium bromide (1 μ L of

a 10 ng/mL solution per 10 mL of agarose gel volume) and the gel was run at 110 volts for 30 minutes. 1X TAE was the gel running buffer and the solvent for the agarose. The gel was viewed with ultraviolet light and documented by digital photography with a Bio-Rad GelDoc XR gel documentation system. Successful encapsulation was determined when the siRNA/liposome complex, which is neutral in charge and is stained by the ethidium bromide, does not travel from the wells where they were loaded. Leakage of siRNA from the liposomes is observed by viewing free siRNA in the body of the agarose gel below the wells. Free liposomes will travel in the direction opposite of the nucleic acids due to their positive charge and leave the agarose gel, yielding no visible results in these lanes.

Determination of Liposome Encapsulation Capacity

To determine the maximum amount of siRNA that could be held by the liposomes, liposomes were prepared with increasing volumes of siRNA, ranging from no siRNA (called “0X”) to the typical formulation (called “1X”), up to 10 times the siRNA used in the “1X” formulation (called “10X”). For each preparation, the same volume (1.3 μ L) of liposomes was used, and the appropriate volumes of diluent (either sterile 0.9% saline or dH₂O) and 20 μ M siRNA were added (Table 2-3). In these experiments, 100% pegylated liposomes were mixed with 0.9% sterile saline as the diluent, while 75% pegylated liposomes were mixed with 0.9% sterile saline or dH₂O as diluents to determine if there was any difference in encapsulation efficiency.

The liposome preparations were incubated at room temperature for one hour, and first visually inspected for sedimentation. 4.3 μ L ghost loading buffer was then added to

each liposome preparation. A free, non-encapsulated siRNA control was prepared by mixing 1.6 μL of 20 μM siRNA, 11.3 μL dH_2O , and 4.3 μL ghost loading buffer. 10 μL of each resulting mixture was loaded into a 2% agarose gel containing ethidium bromide. The gel was run at 110 volts for 30 minutes. 1X TAE was the gel running buffer and the solvent for the agarose. The gel was viewed with ultraviolet light and documented by digital photography with a Bio-Rad GelDoc XR gel documentation system.

***In Vitro* Transfection Methods (Oligofectamine and Liposomes)**

In order to determine the ability of the siRNA molecules to down-regulate gastrin, AsPC-1-Luc cells were first treated with siRNA targeted against position 286 of the gastrin mRNA using the Oligofectamine transfection reagent (Invitrogen). 300,000 cells were seeded in triplicate for each transfection condition into 6-well plates 24 hours before transfection. All transfections using Oligofectamine were done in triplicate according to the manufacturer's directions. After transfection, the plates were returned to the incubator for a 72-hour incubation time where the cells were not disturbed. The 72-hour incubation time was established in our laboratory by an experiment performed with AsPC-1-Luc cells which determined that a 72-hour incubation time yielded the most effective down-regulation of gastrin mRNA. After the 72-hour incubation time, the cells in each well were lysed individually and the RNA extracted as described in the section "RNA Isolation from Cell Culture".

For liposome-mediated transfection of AsPC-1-Luc cells, 300,000 cells were first seeded in triplicate for each transfection condition into 6-well plates 24 hours before

transfection. The following day, 64.5 μ L of the appropriate liposome preparation (containing 100% pegylated liposomes) or sterile 0.9% saline solution was added to 135.5 μ L of complete RPMI 1640 medium containing 10% fetal calf serum. The resulting mixture was then transferred to a 5-mL centrifuge tube containing 2.5 mL of complete medium. The medium was then removed from the cells by aspiration, and replaced with the liposome-containing medium. The plates were returned to the incubator for a 72-hour incubation time where the cells were not disturbed. After the incubation time, the cells in each well were lysed individually and the RNA extracted as described in the section “RNA Isolation from Cell Cultures”.

For liposome-mediated transfection of BxPC-3-Luc cells, 200,000 or 125,000 cells were first seeded in triplicate for each transfection condition into 6-well plates 24 hours before transfection. The following day, 64.5 μ L of the appropriate liposome mixture (containing 75% pegylated liposomes) was added to 135.5 μ L of complete RPMI 1640 medium containing 10% fetal calf serum. The resulting mixture was then transferred to a 5-mL centrifuge tube containing 2.5 mL of complete medium. The medium was then removed from the cells by aspiration, and replaced with the liposome-containing medium. The plates were returned to the incubator for a 72-hour incubation. After the incubation, the cells were lysed as a group of three wells and RNA extracted as described in the section “RNA Isolation from Cell Cultures”.

RNA Isolation from Cell Cultures

RNA isolation from cell cultures was performed using the RNEasy RNA Isolation Kit (Qiagen). RNA isolation was performed according to the manufacturer's directions. For AsPC-1-Luc cells, RNA from cells present in each well was extracted separately. For BxPC-3-Luc cells, the triplicate wells were grouped together at the cell lysis step. After RNA isolation was completed, the RNA samples were diluted 1:50 in RNase-free dH₂O and subjected to spectrophotometric determination of quality and concentration with a Beckman DU 640 spectrophotometer. RNA concentrations were calculated using a Microsoft Excel spreadsheet designed to calculate nucleic acid concentrations. DNase I treatment and endpoint RT-PCR analysis was then performed on these RNA samples as described in the section “DNase I Treatment and Endpoint RT-PCR”. For real-time RT-PCR experiments, RNA samples were subjected to quality analysis and concentration analysis with an Agilent Technologies 2100 Bioanalyzer located in the Hershey Center for Applied Research at the Penn State University College of Medicine. The RNA samples were then subjected to real-time RT-PCR analysis as described in the section “Real-Time RT-PCR”.

DNase I Treatment and Endpoint RT-PCR

To minimize potential PCR contamination by genomic DNA, the RNA samples were subjected to DNase treatment using Amplification Grade DNase I (Invitrogen). 1 µg of each RNA sample was treated with DNase I according to the manufacturer's

instructions.

Endpoint RT-PCR for gastrin and GAPDH (to confirm RNA loading consistency) was then performed on the DNase-treated RNA samples. 200 ng of each RNA sample was mixed with water, the appropriate primer pairs for gastrin (GLM 54 and GLM 55) and GAPDH (GLM 69 and GLM 70) (10 μ M stock concentration, Table 2-4) and then added the appropriate reagents from the Onestep RT-PCR kit (Invitrogen) according to the manufacturer's instructions.

Endpoint RT-PCR was performed in an Eppendorf MasterCycler Gradient thermal cycler using the following series of steps: 60°C for 30 minutes; 94°C for 2 minutes; a variable number of cycles (Table 2-5) of 94°C, 60°C, and 68°C; and a 4°C hold until the samples were either stored or used.

After the endpoint RT-PCR is completed, the PCR products are separated on a 2% agarose gel stained with ethidium bromide (0.5 μ L of a 10 mg/mL ethidium bromide solution in a 100-mL agarose gel, 0.75 μ L in a 150-mL agarose gel). 1X TAE was the solvent for the agarose gel. 2 μ L of loading dye containing bromophenol blue, glycerol, and dH₂O was added to each PCR product and either 10 or 15 μ L was loaded into the gel depending on the size and number of wells present in the gel. The gels were run in 1X TAE gel running buffer stained with 2 μ L ethidium bromide at 110 volts for 80 minutes. The gel was viewed with ultraviolet light and documented by digital photography with a Bio-Rad GelDoc XR gel documentation system.

Real-Time RT-PCR

Real-time RT-PCR analysis was then performed to determine if gastrin mRNA levels were lowered by the anti-gastrin siRNA, confirming results obtained by endpoint RT-PCR. Each RNA sample to be used to real-time RT-PCR was first submitted to quality control analysis using an Agilent Technologies 2100 Bioanalyzer located in the Hershey Center for Applied Research and maintained by the Penn State University College of Medicine Functional Genomics Core Facility. This determined the quality of the RNA and the amount of RNA present in each sample. The amount of RNA was then entered into a Microsoft Excel spreadsheet designed to calculate the required volumes for reverse transcription.

Based on the Microsoft Excel spreadsheet's calculations, the appropriate volume of each RNA sample containing 2 μg of RNA was combined with RNase-free dH_2O for a total sample volume of 10 μL . For each RNA sample, the following components of the High Capacity cDNA Reverse Transcription Kit (Applied Biosystems) were combined as a master mix (volumes listed are for one reverse transcription reaction) for enough volume to do all the reactions plus an error factor of two reactions: (1) 2 μL 10X Reverse Transcription Buffer; (2) 0.8 μL 25X dNTP Mix; (3) 2 μL 10X Random Primers; (4) 1 μL Multiscribe Reverse Transcriptase; (5) 1 μL RNase Inhibitor; and (6) 3.2 μL RNase-free dH_2O . The volumes required for the master mix were scaled up to accommodate all of the RNA samples in an experiment. The 10 μL volume of the RNA/ dH_2O mixture was then mixed with 10 μL of the reverse transcription master mix. Each resulting mixture was transferred to an Eppendorf Mastercycler Gradient thermal cycler for the following

steps: (1) 25⁰C for 10 minutes; (2) 37⁰C for 120 minutes; (3) 85⁰C for 5 seconds; and (4) a 4⁰C hold until samples are stored or used.

Real-time RT-PCR reactions were set up in 384-well plates in triplicate (for AsPC-1-Luc cells) and quadruplicate (for BxPC-3-Luc cells) for both the control (cyclophilin (PPIA)) and target (gastrin) reactions. All RNA samples (now cDNA due to reverse transcription) were diluted with dH₂O to the point where a volume of 4.5 μL used in each real-time PCR reaction contains 100 ng of cDNA. 4.5 μL of each cDNA sample was placed in the appropriate wells of the 384-well plate. 4.5 μL of dH₂O was also used as a negative control. Real-time PCR master mixes for gastrin and the endogenous control cyclophilin were created separately by adding 5 μL of a real-time Master Mix (Applied Biosystems) with 0.5 μL of the appropriate Gene Expression Array (Applied Biosystems) per real-time PCR reaction. 5.5 μL of the Master Mix/Gene Expression Array mixture was added to each RNA sample for a total of 10 μL for each reaction. Once all liquids were added to the 384-well plate, it was covered with a plastic sheet and then with aluminum foil to protect photosensitive elements in the Gene Expression Array. The foil-covered plate was then placed in a plastic bag for further protection. The 384-well plate was transported to the Penn State College of Medicine Functional Genomics Core Facility for real-time PCR analysis using an Applied Biosystems 7900HT Fast Real-Time PCR System. After the raw data was generated from the real-time PCR run, the data was imported to a text file with the SDS 2.2.2 software (Applied Biosystems), and the number of cycles used to obtain the minimum threshold value of fluorescence detected by the real-time PCR system were entered into a Microsoft Excel spreadsheet designed to

calculate if there was any statistical significance in gastrin down-regulation between cells treated with saline and cells treated with liposome/siRNA complexes. Statistical significance was calculated with the same spreadsheet using a pairwise Student's T-Test comparison against saline-treated samples.

Immunocytochemistry

Immunocytochemical analysis was performed on liposome-treated BxPC-3-Luc cells to determine if the anti-gastrin siRNA also down-regulated the expression of the gastrin peptide. 300,000 BxPC-3-Luc cells were plated in duplicate in 6-well plates containing glass microscope cover slips. Cells were treated with the appropriate liposome/siRNA mixture, empty liposomes, or saline as described in the section “*In Vitro* Transfection Methods”. After the 72-hour incubation time, the media was removed by aspiration and the cells fixed to the coverslips with 100% ice-cold methanol. The 6-well plates were then moved to a -20°C freezer until analysis. The coverslips were removed from the methanol and transferred to a 12-well plate containing acetone to wash the coverslip. Nonspecific binding was blocked with SPB (Sorenson’s Phosphate Buffer) containing 3% FBS and 0.1% Triton-X-100 for 1 hour. The coverslips were then incubated in SPB containing a rabbit polyclonal gastrin antibody (T-4347, Peninsula Labs, Carlsbad, CA) at a titer of 1:1,000 overnight at 4°C. After three washes in SPB containing 1% FBS, the coverslips were incubated in SPB containing 3% FBS, 0.1% Triton-X-100 and the secondary rhodamine-labeled goat anti-rabbit antibody (1:2,000 titer) (Amersham Biosciences) for 2 hours at 4°C in the dark. The coverslips were

washed twice with SPB for 30 minutes each and mounted with Aqua Poly/Mount solution (Polysciences). Controls for this experiment included liposome-treated and non-liposome-treated BxPC-3-Luc cells treated with secondary antibody alone.

***In Vitro* Growth Study**

To determine the effects of anti-gastrin siRNA on the growth rates of the BxPC-3-Luc cell line, an *in vitro* growth study was performed. 24 hours before transfection with liposome/siRNA complexes, 20,000 cells were seeded into 25-mm² cell culture flasks containing 5 mL of complete medium. Cells were seeded in triplicate for 5 time points for the following treatments: (1) 0.9% saline, (2) empty liposomes, (3) scrambled control si90 siRNA, and (4) target si90 siRNA. This was a total of 15 flasks for each treatment. Liposomes were prepared based on the formulation described in “Encapsulation of siRNA into Liposomes”, and 5.2 µL of the appropriate treatment was added to each flask, and the flasks were returned to the incubator until collected for counting. For cell counting, the cells were treated with 0.5 mL 0.25% trypsin/EDTA solution (Invitrogen) and returned to the incubator to release from the flask, usually around 5 minutes after treatment. 0.5 mL of complete medium was then added to deactivate the trypsin, and 20 µL of the resulting mixture was removed and transferred to a 0.65-mL microcentrifuge tube. 20 µL of 0.4% Trypan Blue stain (Invitrogen) was then added to the cells, and the cells were counted using a hemacytometer. The cells present in the four corners of the hemacytometer were counted and the average of the corners was used to calculate the cell count in each flask. Cell counts were taken 2, 6, 8, 9, and 10 days after liposome

treatment. At the end of the growth study, the average cell counts and the standard deviations for each treatment at each time point were calculated and graphed on a Microsoft Excel spreadsheet. Statistical significance was determined using a pairwise Student's T-Test compared against saline-treated cells.

***In Vivo* Orthotopic Model of Pancreatic Cancer**

To determine the *in vivo* effects of the liposome-mediated siRNA delivery system on pancreatic tumors, an orthotopic model of pancreatic cancer was established. 6-week old male athymic nude mice (Charles River Laboratories) were kept in sterile conditions at the Penn State University College of Medicine Animal Research Facility and fed with the appropriate diet and water in accordance with the AAACCR guidelines for veterinary medicine. The research protocol was approved by the Institutional Animal Care and Usage Committee of the Pennsylvania State University College of Medicine. The mice were maintained in cages of no more than 6 mice, with dominant mice kept in isolation. To establish the orthotopic tumors, the mice were first anesthetized with a mixture of Ketamine-HCl (129 mg/kg mouse mass) and Xylazine (4 mg/kg mouse mass), the pancreas exposed by surgical incision into the peritoneum, and then 1×10^6 BxPC-3-Luc cells were injected the pancreas using a syringe attached to a 27-gauge needle. The incision was closed by wound clips which were removed once the incision was healed, a period of between 7 and 14 days after the orthotopic injections were performed.

Luciferase Imaging of Mouse Orthotopic Tumors

To determine the size and the activity level of the tumor, luciferase imagery was performed on the mice carrying the orthotopic BxPC-3-Luc tumors. BxPC-3-Luc cells produce the luciferase enzyme, which emits light when ATP and the enzyme's substrate luciferin are present. Mice were anesthetized with 100 to 200 μ L of a mixture of Ketamine-HCl (129 mg/kg mouse mass) and Xylazine (4 mg/kg mouse mass) given via intramuscular injection into the left thigh. When the mice are sufficiently anesthetized (usually between 5 and 10 minutes after injection), 100 μ L of a luciferin solution (Nanolight Technologies) at the concentration of 135 mg luciferin/kg mouse mass in sterile 1X DPBS, was administered via intraperitoneal injection. The mice were then left for 10 minutes while the luciferase enzyme in the BxPC-3-Luc cells metabolizes the luciferin, producing light. The mice were then placed on their backs inside the IVIS imaging system (Xenogen), and photographed for an exposure time of between 5 seconds and 1 minute, depending on the intensity of light produced by the BxPC-3-Luc cells. The intensity of light produced by the BxPC-3-Luc cells (called the relative flux) was then measured and quantified by the Igor Pro software (Xenogen). Mice were first imaged one week after initial orthotopic injections to establish liposome/siRNA treatment groups, and then the mice were imaged once a week after the start of liposome/siRNA treatments until the conclusion of the study.

Randomization of Mice into Treatment Groups

After the first round of imaging of mouse tumors, the mice were organized based on the relative intensity of the light emitted from the BxPC-3-Luc cells. The mice were then sorted at random into the following treatment groups: (1) 0.9% sterile saline solution, (2) empty (ghost) liposomes, (3) liposome-encapsulated scrambled control si90 siRNA, (4) liposome-encapsulated target si90 siRNA, (5) liposome-encapsulated scrambled control si286 siRNA, and (6) liposome-encapsulated target si286 siRNA. At the beginning of the liposome treatments, there were 10 mice in group 1, 11 mice in group 2, and 9 mice in groups 3 through 6. Each group of mice had a similar average luciferase intensity.

Preparation of Liposomes and Injection of Liposomes into Mice

The liposome preparations were generated as described in the section “Encapsulation of siRNA into Liposomes and Confirmation of Loading”, with a final volume sufficient for injection of 100 μ L of liposomes into each group of mice. Before the liposomes were injected into the mice, liposome encapsulation was tested by visual inspection and agarose electrophoresis as described in the section “Encapsulation of siRNA into Liposomes and Confirmation of Loading”. When successful liposome encapsulation of siRNA was confirmed by visual inspection and electrophoresis, the liposomes were taken to the Penn State University Animal Research Facility, where the mice were located. The cages were covered with a sterile transport cover and removed

from the sterile storage chamber. The mice were then moved to a sterile laminar flow hood designed for animal work and the mice placed in a tailveiner (Braintree Scientific) that held the mice in place while exposing the tail. The tail was heated under a lamp for between 30 seconds and 1 minute to expose the lateral tail vein. 100 μ L of the appropriate liposome/siRNA mixture (or 0.9% sterile saline solution) was then injected into the lateral tail vein with a syringe attached to a 21-gauge needle. Successful injection was observed by visual confirmation of the liposomes entering the circulation and not forming a bolus at the injection site. After injections were completed, the mice were returned to their cages, covered with a sterile transport cover, and returned to the sterile storage chamber. Injections of liposomes occurred three times a week on Monday, Wednesday, and Friday for eight weeks.

Sacrificing and Removal of Tissues From Mice

After the completion of the liposome treatments on the mouse orthotopic tumors when the tumor burden on the saline solution-treated mice became too large, the mice were sacrificed. The mice were first anesthetized by exposure to carbon dioxide and then weighed. This was followed by cardiac puncture, which sacrificed the mice, and collection of blood. The mice were then dissected and examined for signs of metastasis. The pancreatic tumors were removed and weighed. The following organs were removed, weighed, and stored in a 10% neutral buffered formalin solution for future pathological study: The pancreas, gastrointestinal tract (the stomach and intestines), spleen, kidneys, lungs, and heart. The skin was removed from the head, the head removed from the rest of

the body, and stored in Formical-4 solution (Decal Chemical). The remainder of each mouse carcass was stored in 10% neutral buffered formalin along with the organs, but was not weighed.

Analysis of Effects of Liposome Treatment on Orthotopic Tumors

Tumor tissues were sectioned and RNA was isolated from each mouse tumor using the RNEasy RNA Isolation Kit (Qiagen), according to the manufacturer's instructions. The RNA samples were then submitted for quality control analysis, and real-time RT-PCR for gastrin and cyclophilin (PPIA) performed as described in the section “Real-Time RT-PCR”.

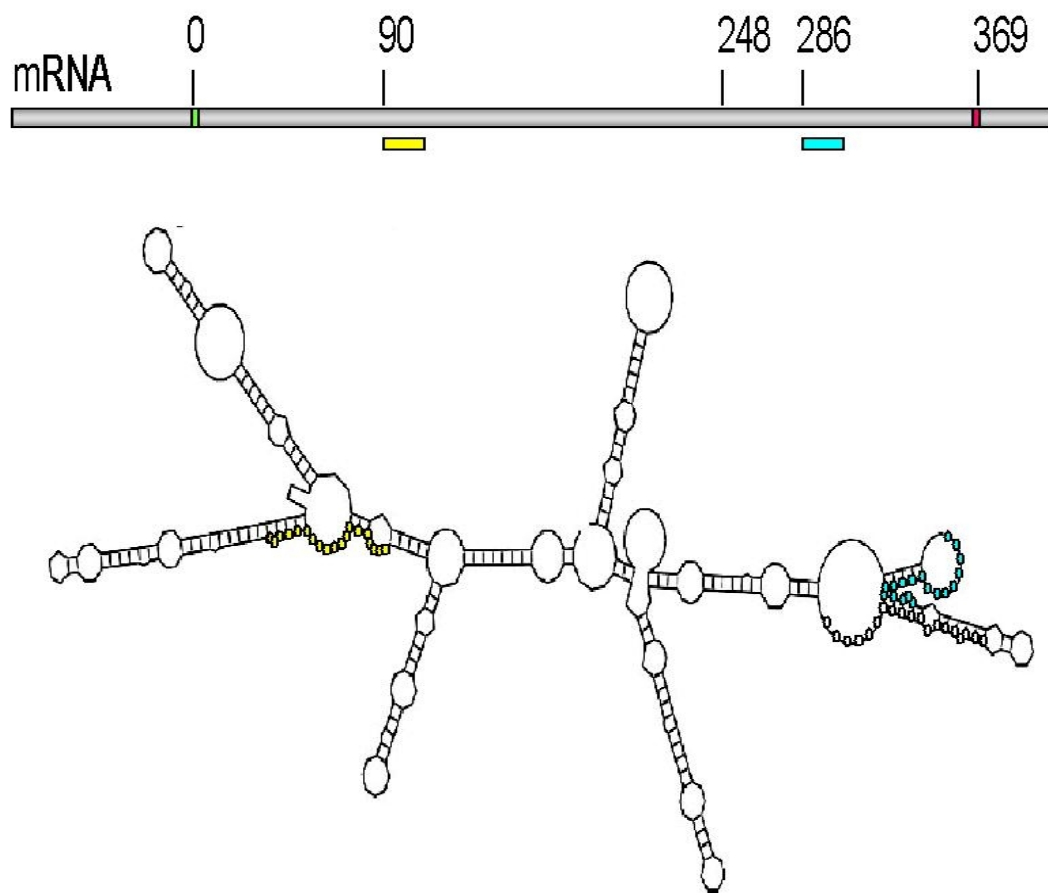


Figure 2-1: Target sites on the gastrin mRNA of the siRNA molecules used.

Table 2-1: Nucleotide sequences of the siRNA molecules used.

SiRNA Name	Sequence (5' to 3')
Si90 Target	CUGUACCUAAGGGUGCAUCUGGCUG
Si90 Scrambled Control	CUGGGAUUCCGAAUGGACGUCUCUG
Si286 Target	GCCGCAGUGCUGAGGAUGAGAACUA
Si286 Scrambled Control	GCCUGAUCGGAGUAGGAGAAGCCUA

Table 2-2: Formulations for one in vitro liposome encapsulation of siRNA with control treatments (all volumes are in μL). Note: All volumes can be scaled up for multiple treatments.

Condition	0.9% Saline	siRNA (20 μM)	Liposomes (25 mg/mL)	Total Volume
Saline only	64.5	0	0	64.5
Empty (Ghost) Liposomes	58	0	6.5	64.5
Liposomes and siRNA	50	8	6.5	64.5

Table 2-3: Formulations for liposome capacity test (all volumes are in μL).

Condition	0.9% Saline or dH ₂ O	siRNA (20 μM)	Liposomes (25 mg/mL)	Total Volume
Empty (Ghost) Liposomes	21.6	0	0	21.6
1X	20	1.6	1.3	21.6
2X	18.4	3.2	1.3	21.6
3X	16.8	4.8	1.3	21.6
4X	15.2	6.4	1.3	21.6
5X	13.6	8	1.3	21.6
6X	12	9.6	1.3	21.6
7X	10.4	11.2	1.3	21.6
8X	8.8	12.8	1.3	21.6
9X	7.2	14.4	1.3	21.6
10X	5.6	16	1.3	21.6

Table 2-4: Endpoint PCR primers for gastrin and GAPDH. The primer pair GLM 54 and 55 yield a PCR product of 273 base pairs with a genomic DNA product of 403 base pairs, and the primer pair GLM 69 and 70 yield a PCR product of 537 base pairs with no genomic DNA product.

Primer Name	PCR Target	Nucleotide Sequence (5' to 3')
GLM 54	Gastrin (forward)	CAGCGACTATGTGTGTATGTGCTG
GLM 55	Gastrin (reverse)	GAAGTCCATCCATCCATAGGC
GLM 69	GAPDH (forward)	GTGAAGGTCGGAGTCAACGGATT
GLM 70	GAPDH (reverse)	AGTGATGGCATGGACTGTGGTC

Table 2-5: PCR cycles required for endpoint PCR of gastrin and GAPDH. The cycle numbers are variable due to differences between the cell lines and transfection conditions.

Cell Line	PCR Target	Number of PCR Cycles (Transfection Conditions)
AsPC-1-Luc	Gastrin	29 (300,000 cells, Oligofectamine); 28 (300,000 cells, all liposome transfections)
AsPC-1-Luc	GAPDH	22 (all conditions)
BxPC-3-Luc	Gastrin	35 (200,000 cells, liposomes); 37 (125,000 cells, liposomes)
BxPC-3-Luc	GAPDH	22 (all conditions)

Chapter 3

Results

100% and 75% pegylated liposomes have different siRNA loading capacities.

Liposomes with 100% and 75% pegylation were tested for siRNA loading capacities due to their differing uptake rates in the AsPC-1-Luc and BxPC-3-Luc cell lines. To determine the siRNA encapsulation capacity of liposomes, an increasing series of siRNA concentrations were mixed with a constant amount of liposomes. 100% pegylated liposomes were diluted in 0.9% sterile saline, while 75% pegylated liposomes were diluted in 0.9% sterile saline or dH₂O. After the one-hour incubation time, the liposomes were visually inspected for signs of sedimentation (called “crashing out”), and then subjected to agarose electrophoresis. Any sedimentation would signify a loss of ability to successfully perform liposome-mediated transfection *in vitro* and *in vivo*. In 100% pegylated liposomes, sedimentation occurred beginning at the 6X siRNA amount (Table 3-1). In 75% pegylated liposomes, sedimentation began at the 4X siRNA amount for liposomes prepared in saline and at the 5X siRNA amount for liposomes prepared in dH₂O (Table 3-2).

After the visual sedimentation inspection was completed, the liposome/siRNA mixtures were then resolved by electrophoresis on a 2% agarose gel stained with ethidium bromide to further determine loading capacity. Any leaking out of siRNA would signify loss of liposome-mediated transfection efficiency *in vitro* or *in vivo*,

because naked siRNA is not stable in serum (63, 64, 65). In 100% pegylated liposomes diluted in 0.9% sterile saline, siRNA began to leak out at the 4X siRNA amount (Figure 3-1). In 75% pegylated liposomes diluted in 0.9% sterile saline, leakage began at the 5X siRNA amount (Figure 3-2A), while liposomes diluted in sterile RNase-free water exhibited leakage beginning at the 4X siRNA amount (Figure 3-2B). The sedimentation and electrophoresis data established a maximum amount of siRNA that can be encapsulated by the 100% and 75% pegylated liposomes, and served as a baseline for future experiments using liposomes.

Oligofectamine-mediated and liposome-mediated transfections of anti-gastrin siRNA down-regulate gastrin mRNA in AsPC-1-Luc cells.

To determine if the siRNA targeted against position 286 of the gastrin mRNA was effective at down-regulating gastrin mRNA, we transfected this siRNA into AsPC-1-Luc cells using the Oligofectamine transfection reagent. 300,000 cells in each well of a 6-well plate were treated with saline, empty liposomes, liposome/scrambled control siRNA, and liposome/target siRNA for 72 hours. After the 72-hour treatment, the RNA was extracted from the cells and subjected to spectrophotometer analysis of concentration. Endpoint RT-PCR for gastrin and GAPDH (as a loading control) were then performed on RNA isolated from the cells in each individual well and the resulting PCR products resolved on a 2% agarose gel stained with ethidium bromide. The anti-gastrin siRNA targeted against position 286 was able to down-regulate gastrin mRNA in AsPC-1-Luc

cells while scrambled control siRNA and saline controls did not exhibit down-regulation of gastrin mRNA (Figure 3-3). Endpoint RT-PCR for GAPDH was also performed to ensure consistency of loading of the RNA samples (Figure 3-4).

When it was established the the siRNA could down-regulate gastrin mRNA in AsPC-1-Luc cells, the same experiment was performed with 100% pegylated liposomes as the transfection reagent. Gastrin mRNA down-regulation was observed with the 3X liposome/siRNA formulation (Figure 3-7) but not the 1X liposome/siRNA formulation (Figure 3-5). Endpoint RT-PCR for GAPDH was also performed for both conditions to ensure consistency of RNA samples (Figures 3-6, 3-8).

To confirm the endpoint RT-PCR results showing down-regulation of gastrin mRNA with the 1X and 3X siRNA/liposome formulations, real-time RT-PCR was performed on the same RNA samples. The data obtained from the real-time RT-PCR confirmed the data obtained by endpoint RT-PCR for the 3X formulation when compared to the saline control (Figure 3-9).

Liposome-mediated transfection of anti-gastrin siRNA down-regulates gastrin mRNA in BxPC-3-Luc cells.

Because BxPC-3-Luc cells produce gastrin, this cell line was also a candidate for liposome-mediated anti-gastrin siRNA treatment along with the AsPC-1-Luc cell line. 200,000 and 125,000 cells were treated with the same volumes of liposome/siRNA mixtures that were used for liposome treatments on 300,000-cell AsPC-1-Luc cells.

SiRNAs targeted against positions 90 and 286 of the gastrin mRNA were used. After the 72-hour incubation time, cell lysates from each triplicate treatment were grouped and RNA isolation performed. This was followed by spectrophotometer analysis and endpoint RT-PCR for gastrin and GAPDH. Endpoint RT-PCR revealed down-regulation of gastrin mRNA in both the 200,000-cell (Figure 3-10) and 125,000-cell treatment conditions (Figure 3-12), although the down-regulation was clearer in the 200,000-cell treatment condition. GAPDH RT-PCR revealed consistency among the RNA samples for both the 200,000-cell (Figure 3-11) and 125,000-cell treatment conditions (Figure 3-13)

To confirm the findings obtained by endpoint RT-PCR, real-time RT-PCR was performed on the same RNA samples. For the 200,000-cell treatments, real-time RT-PCR was repeated three times. Real-time RT-PCR revealed that while down-regulation of gastrin mRNA occurred with siRNA targeting both positions 90 and 286 of the gastrin mRNA, statistical significance was obtained with only the siRNA targeted against position 286 (Figure 3-14). For the 125,000-cell treatment condition, real-time RT-PCR was repeated two times. Down-regulation of gastrin mRNA was obtained with the siRNA targeting both positions 90 and 286 of the gastrin mRNA, but the down-regulation did not reach statistical significance in either case, and was more evident for the siRNA targeting position 286 of the gastrin mRNA (Figure 3-15).

Liposome-mediated transfection of anti-gastrin siRNA against position 286 of the gastrin mRNA down-regulates gastrin peptide in BxPC-3-Luc cells.

While endpoint and real-time RT-PCR suggests that liposome-mediated transfection of anti-gastrin siRNA can down-regulate gastrin mRNA in two pancreatic cancer cell lines, we decided to determine if siRNA treatment also causes down-regulation of the gastrin peptide, which could be a possible additional effect of siRNA treatments. 200,000 BxPC-3-Luc cells seeded in wells on top of glass microscope cover slips were treated separately with liposomes containing siRNA targeted against position 286 of the gastrin mRNA. Immunocytochemical analysis and viewing of liposome/siRNA-treated cells on a fluorescent microscope suggested that the siRNA targeted against position 286 of the gastrin mRNA also down-regulated gastrin peptide in BxPC-3-Luc cells without any nonspecific binding of the rhodamine-labeled secondary antibody occurring (Figure 3-16).

Liposome-mediated transfection of siRNA targeted to position 90 of the gastrin mRNA inhibits the growth of BxPC-3-Luc cells.

Since it has been suggested by this series of experiments that liposome-mediated siRNA treatment of pancreatic cancer cells can down-regulate gastrin mRNA and peptide, the next step of the study would be to determine if the same treatment also inhibits the growth of pancreatic cancer cells *in vitro*. BxPC-3-Luc cells were treated with liposome-encapsulated siRNA against position 90 of the gastrin mRNA. The growth study was

performed for 10 days after liposome/siRNA treatment, with cell counts taken 2, 6, 8, 9, and 10 days after transfection. The results of the study suggest that liposome treatment inhibits the growth of BxPC-3 cells (Figure 3-17). However, the data is not statistically significant due to large variations in the cell counts. The results also suggest that liposome-containing media should be replaced before 8 days after initial liposome transfection because of the amount of waste products present in the media, causing cell death and variations in the cell counts at and past the 8-day mark.

Liposome treatment in athymic nude mice does not exhibit toxic effects.

To determine if liposome-mediated siRNA treatment impacted the growth of orthotopic BxPC-3-Luc pancreatic tumors in athymic nude mice, empty liposomes, 0.9% sterile saline, liposome/control siRNA, or liposome/target siRNA mixtures were given to the mice three times a week via injections into the lateral tail vein of the mice.

Liposomes were chosen as the delivery vehicle because they were believed to be nontoxic to animals and delivering nonmodified siRNA can have toxic effects once in the bloodstream (87, 88, 90). After eight weeks of liposome treatments, the mice were sacrificed and the tumors, organs, and tissues harvested for pathological and toxicology analysis. The liver enzymes were subjected to analysis of the liver enzymes (add names of enzymes). The analysis suggested that the liver enzyme levels were not significantly different in the liposome-treated mice when compared to mice treated with saline solution, meaning that the liposome treatments were not toxic to the mice (Table 3-4).

Liposome-mediated siRNA treatment against orthotopic BxPC-3-Luc tumors in athymic nude mice does not significantly reduce gastrin mRNA or inhibit tumor growth.

After the orthotopic tumors were harvested from the mice, the tumors were weighed and each group was compared to the saline control to determine if liposome-mediated siRNA treatment inhibited the growth of the orthotopic tumors. Statistical analysis of tumor masses suggested that neither the siRNA treatments targeted against position 90 nor position 286 of the gastrin mRNA significantly inhibited the growth of the orthotopic tumors when compared to saline controls (Figure 3-18).

RNA was also extracted from the tumors and real-time RT-PCR performed to determine if liposome-mediated siRNA treatment down-regulated the gastrin mRNA levels of the orthotopic tumors. Analysis of the real-time RT-PCR data suggested that gastrin mRNA levels in the orthotopic tumors were not significantly down-regulated by either of the siRNAs used in the study when compared to saline controls (Figure 3-19).



Figure 3-1: Electrophoresis showing 100% pegylated liposome loading capacity. Sterile 0.9% saline was the diluent for the liposomes.

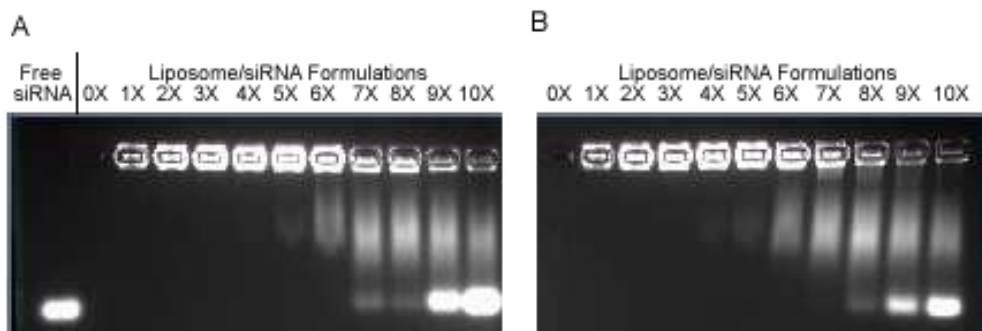


Figure 3-2: Electrophoresis showing 75% pegylated liposome loading capacity in sterile 0.9% saline (A) and dH₂O (B). Electrophoresis for both loading conditions was performed on the same gel.

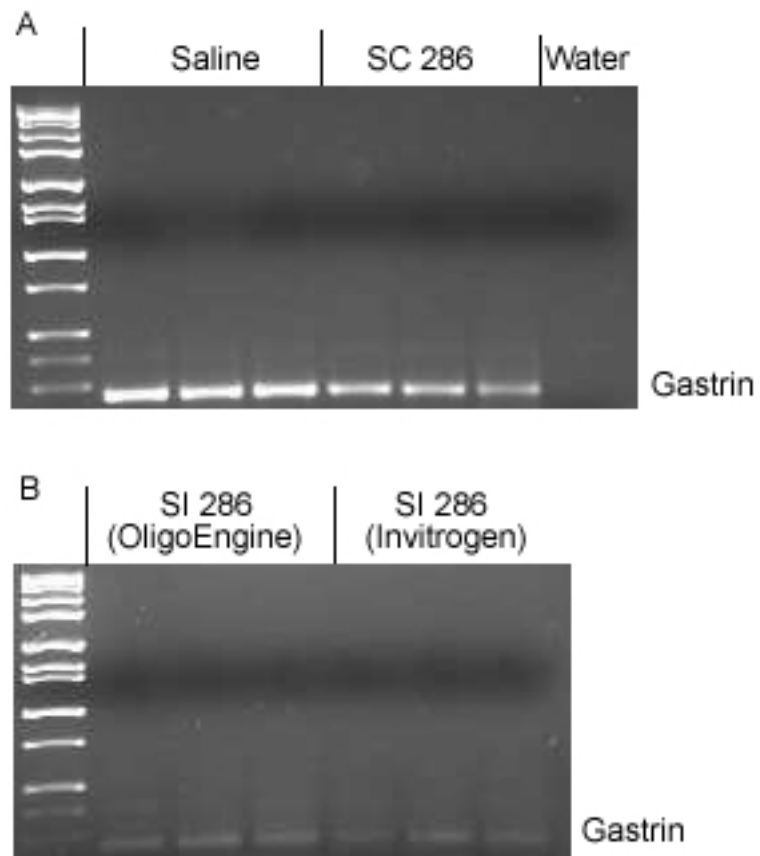


Figure 3-3: Endpoint RT-PCR for gastrin of RNA isolated from Oligofectamine-treated AsPC-1-Luc cells.

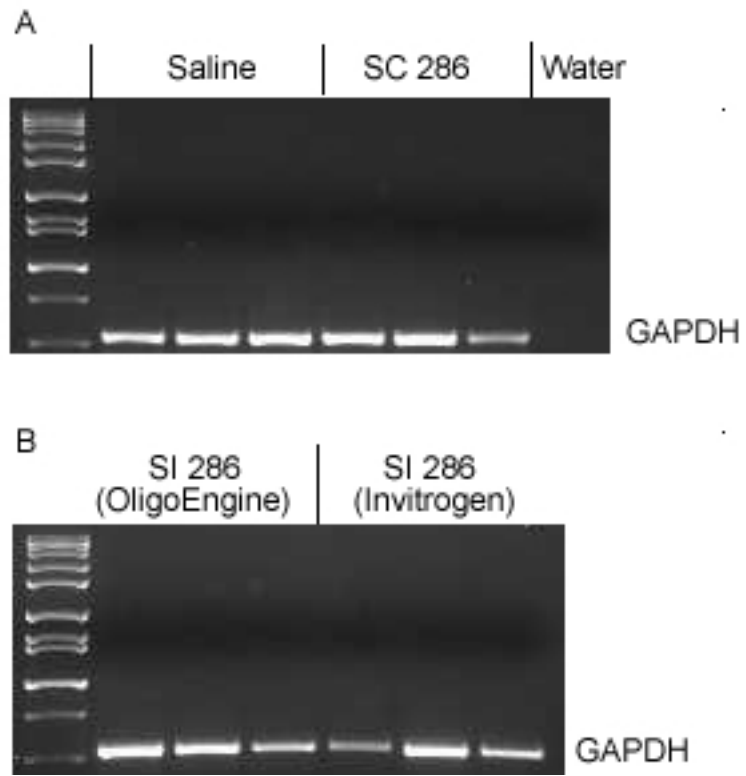


Figure 3-4: Endpoint RT-PCR for GAPDH of RNA isolated from Oligofectamine-treated AsPC-1-Luc cells.



Figure 3-5: Endpoint RT-PCR for gastrin of RNA isolated from liposome-treated AsPC-1-Luc cells, 1X liposome/siRNA formulation.

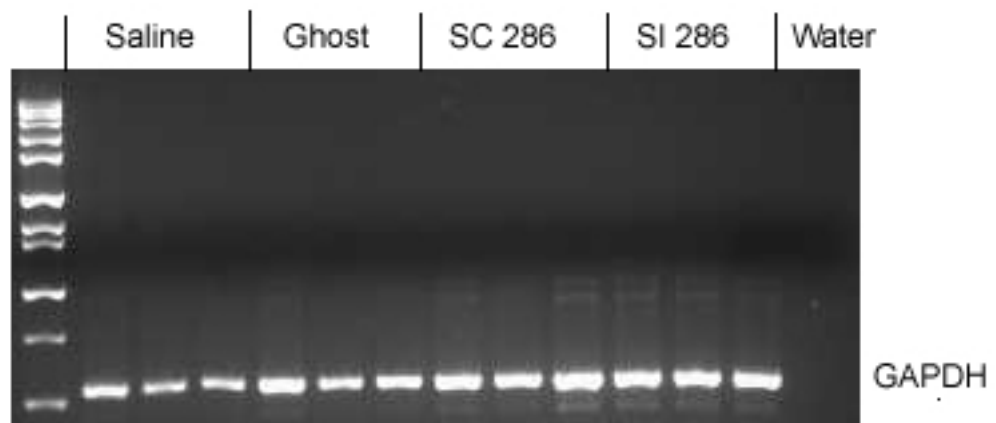


Figure 3-6: Endpoint RT-PCR for GAPDH of RNA isolated from liposome-treated AsPC-1-Luc cells, 1X liposome/siRNA formulation.

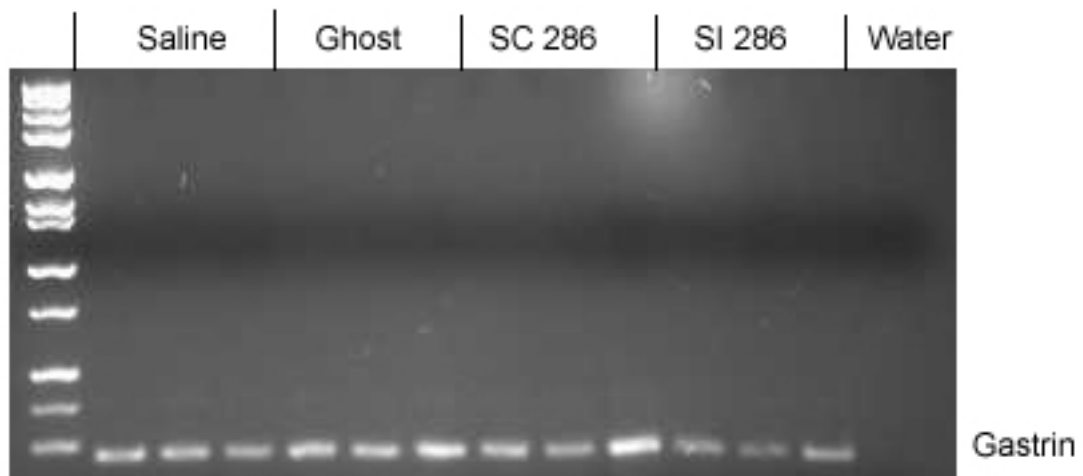


Figure 3-7: Endpoint RT-PCR for gastrin of RNA isolated from liposome-treated AsPC-1-Luc cells, 3X liposome/siRNA formulation.

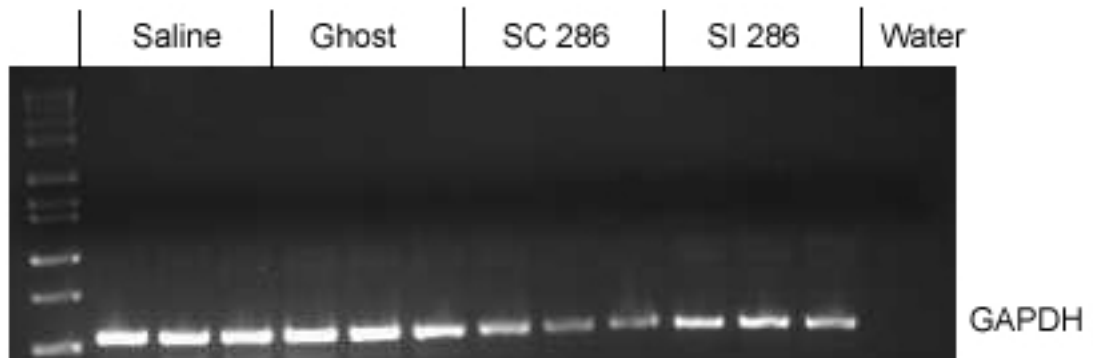


Figure 3-8: Endpoint RT-PCR for GAPDH of RNA isolated from liposome-treated AsPC-1-Luc cells, 3X liposome/siRNA formulation.

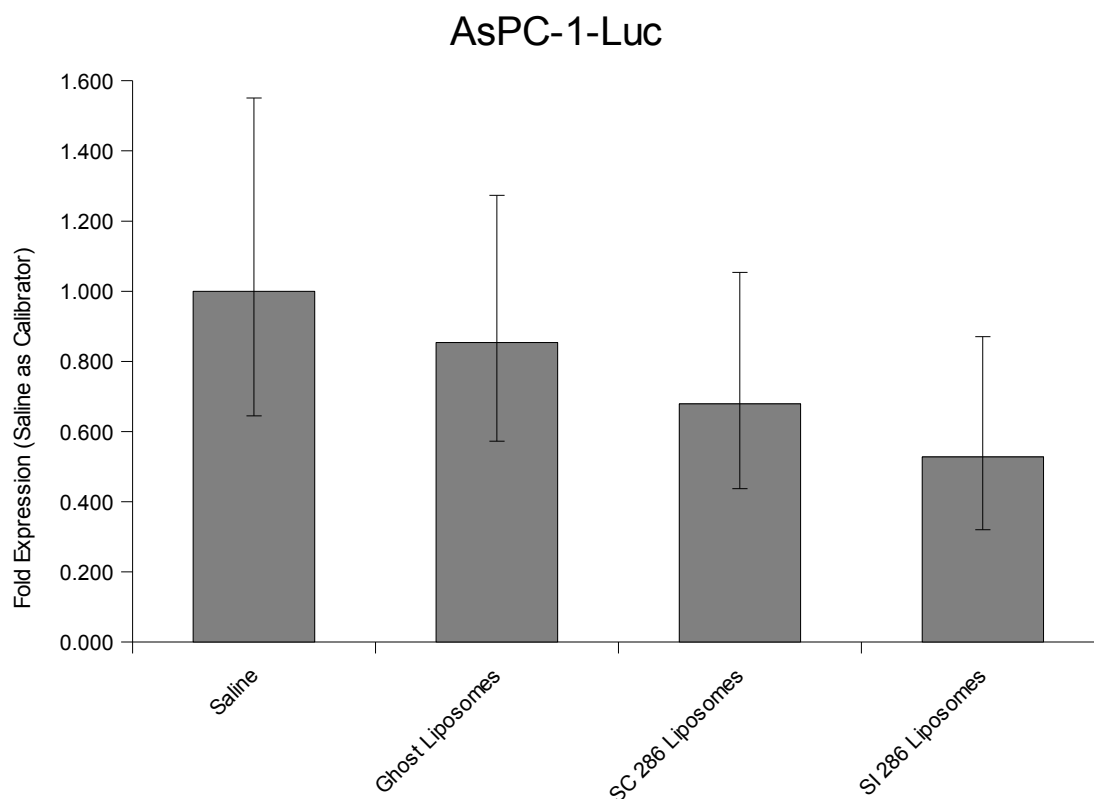


Figure 3-9: Real-time RT-PCR for gastrin of RNA isolated from liposome-treated AsPC-1-Luc cells, 3X liposome/siRNA formulation and 300,000 cells per treatment. Graphs show relative quantity \pm the minimum and maximum relative quantities. Compared to the saline calibrator, SI 286 liposomes achieved down-regulation of gastrin mRNA at a $P=0.0501$ significance level by Student's T-test.

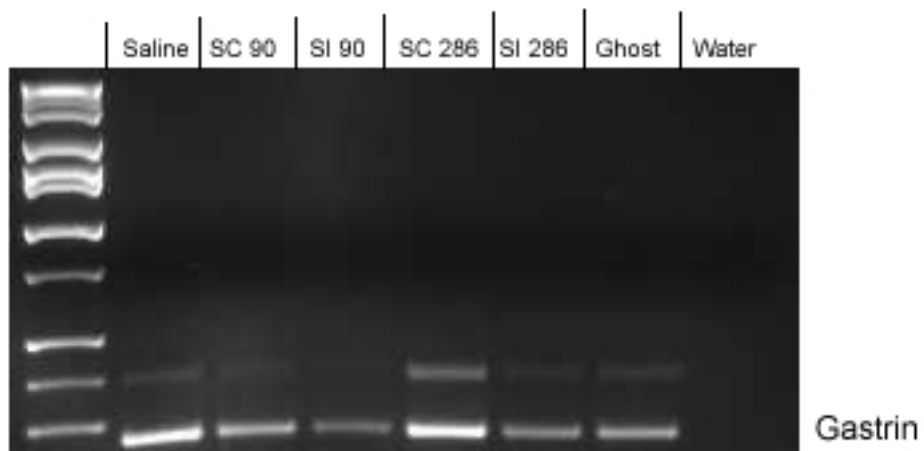


Figure 3-10: Endpoint RT-PCR for gastrin of RNA isolated from liposome-treated BxPC-3-Luc cells, 200,000 cells per treatment.

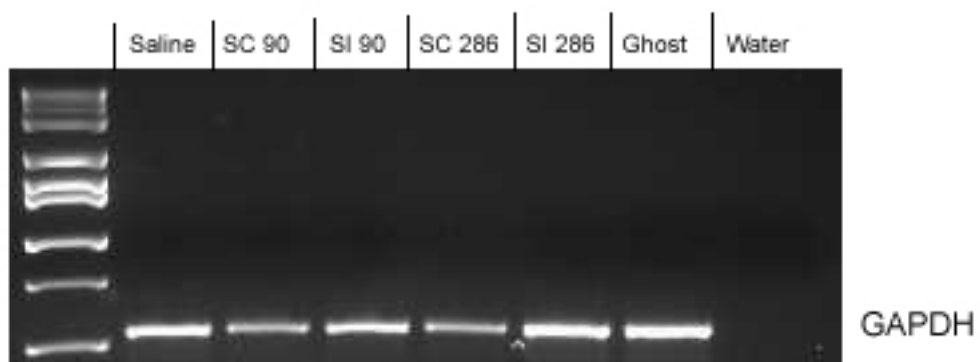


Figure **3-11**: Endpoint RT-PCR for GAPDH of RNA isolated from liposome-treated BxPC-3-Luc cells, 200,000 cells per treatment.

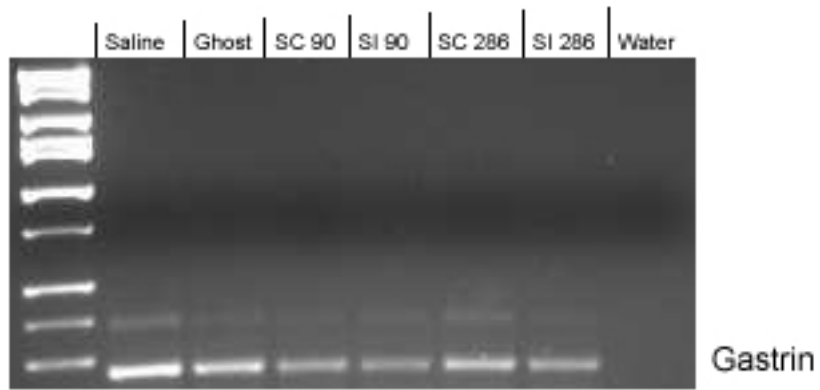


Figure 3-12: Endpoint RT-PCR for gastrin of RNA isolated from liposome-treated BxPC-3-Luc cells, 125,000 cells per treatment.

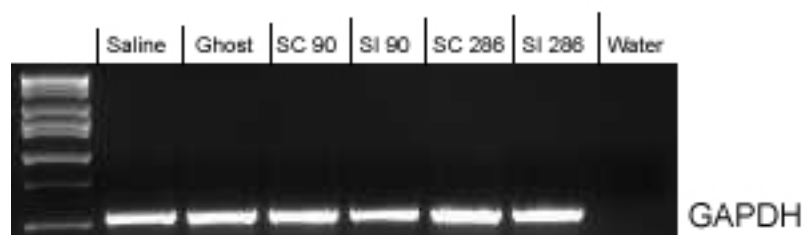


Figure **3-13**: Endpoint RT-PCR for GAPDH of RNA isolated from liposome-treated BxPC-3-Luc cells, 125,000 cells per treatment.

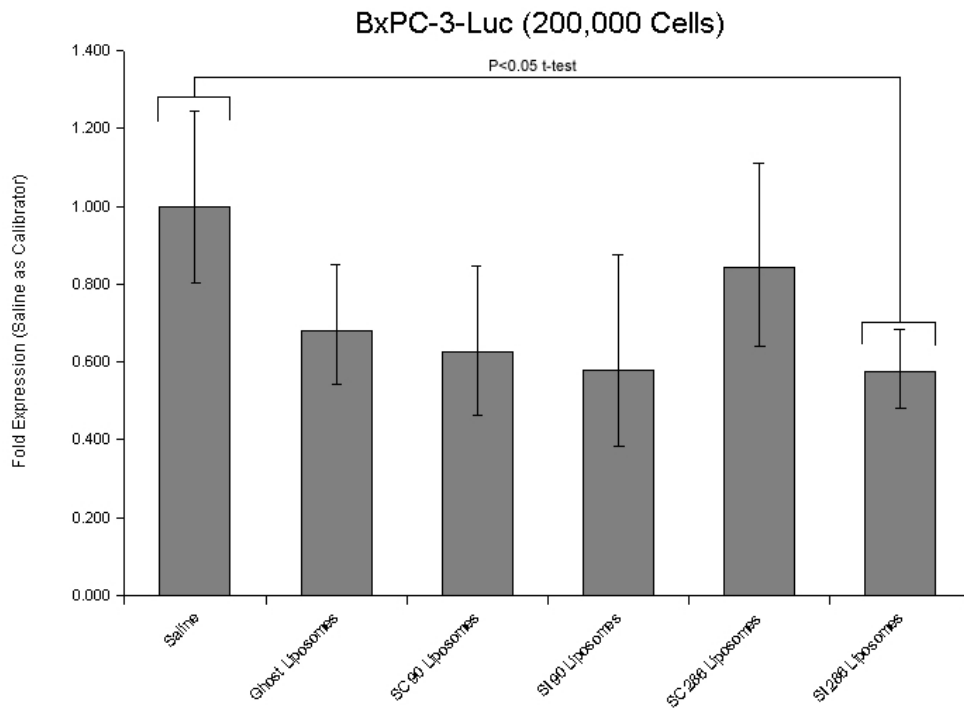


Figure 3-14: Real-time RT-PCR for gastrin of RNA isolated from liposome-treated BxPC-3-Luc cells, 200,000 cells per treatment. Graphs show average relative quantity \pm the maximum and minimum relative quantities (three replicates).

BxPC-3-Luc (125,000 Cells)

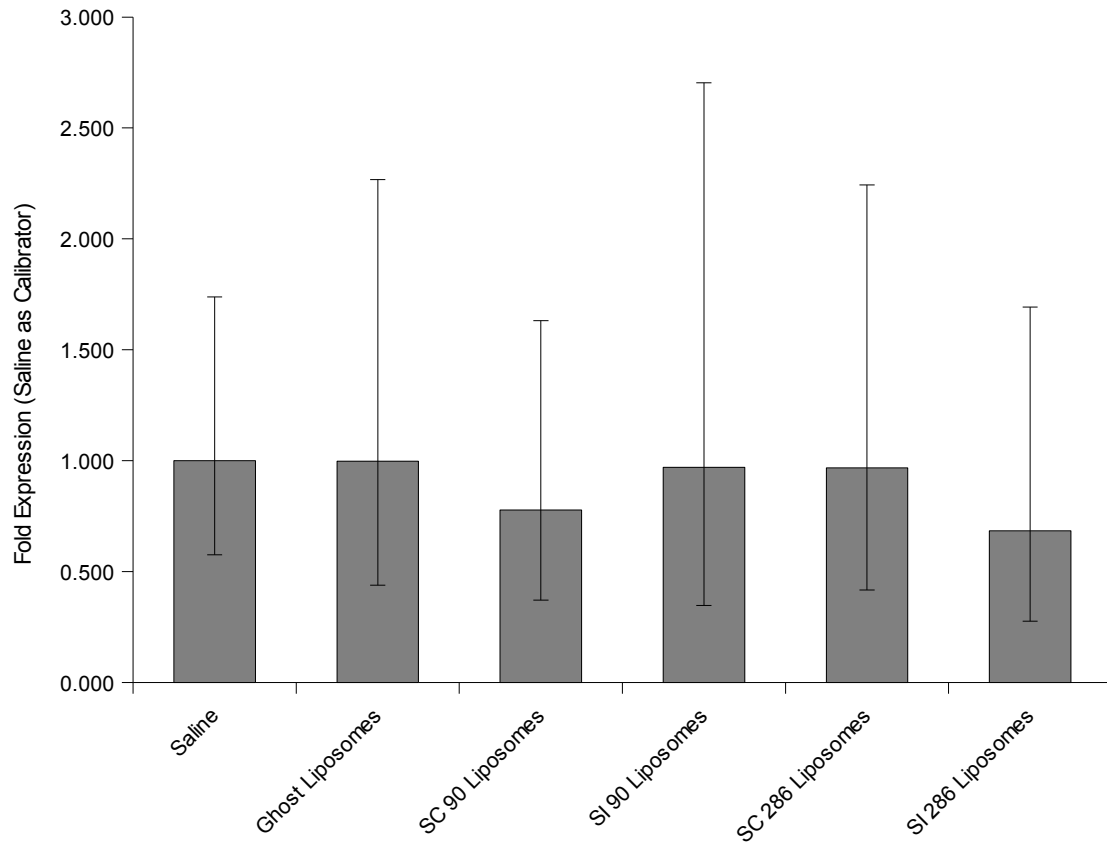


Figure 3-15: Real-time RT-PCR for gastrin of RNA isolated from liposome-treated BxPC-3-Luc cells, 125,000 cells per treatment. Graphs show average relative quantity \pm the maximum and minimum relative quantities (two replicates).

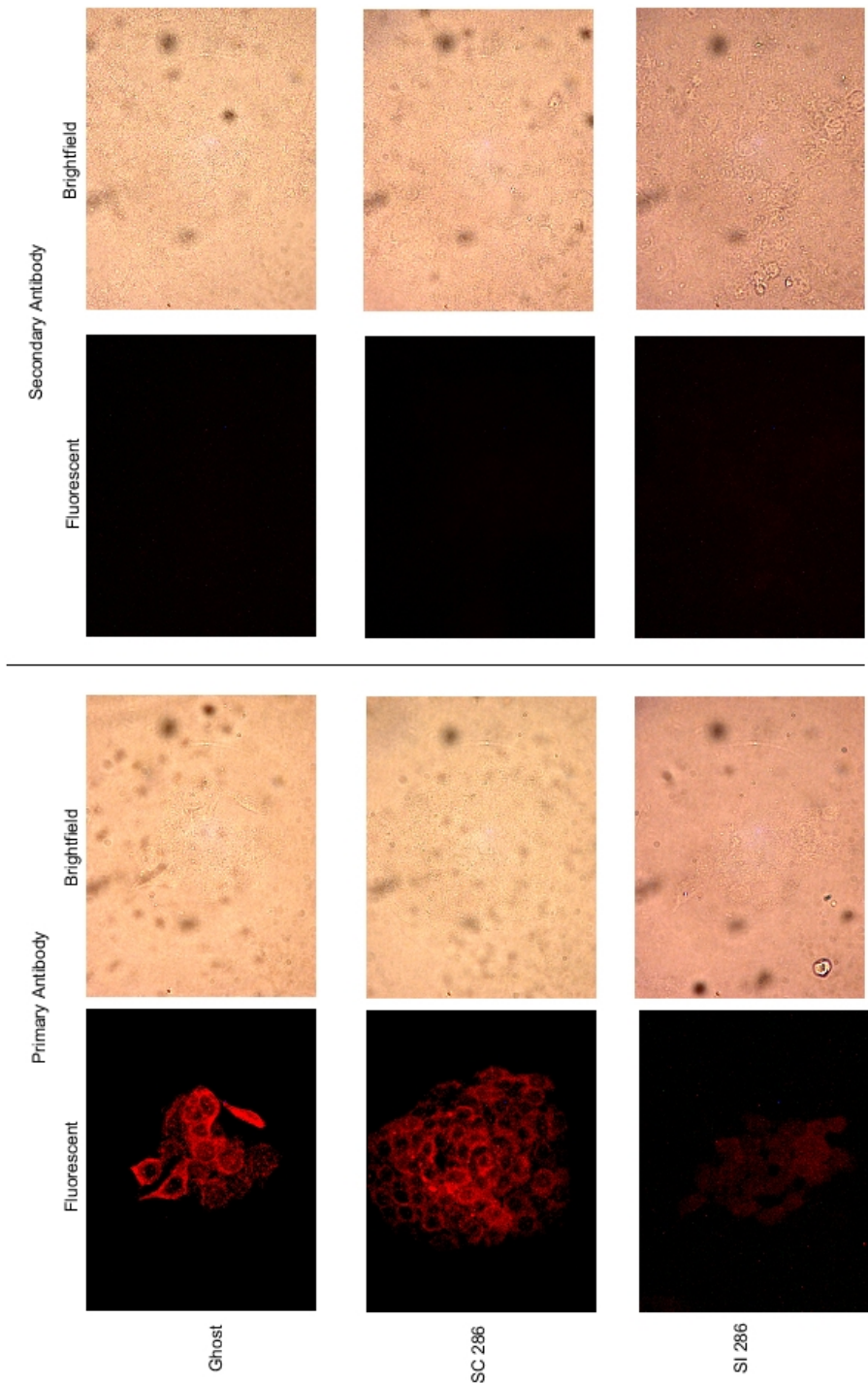


Figure 3-16: Immunocytochemical analysis of liposome/siRNA-treated BxPC-3-Luc cells.

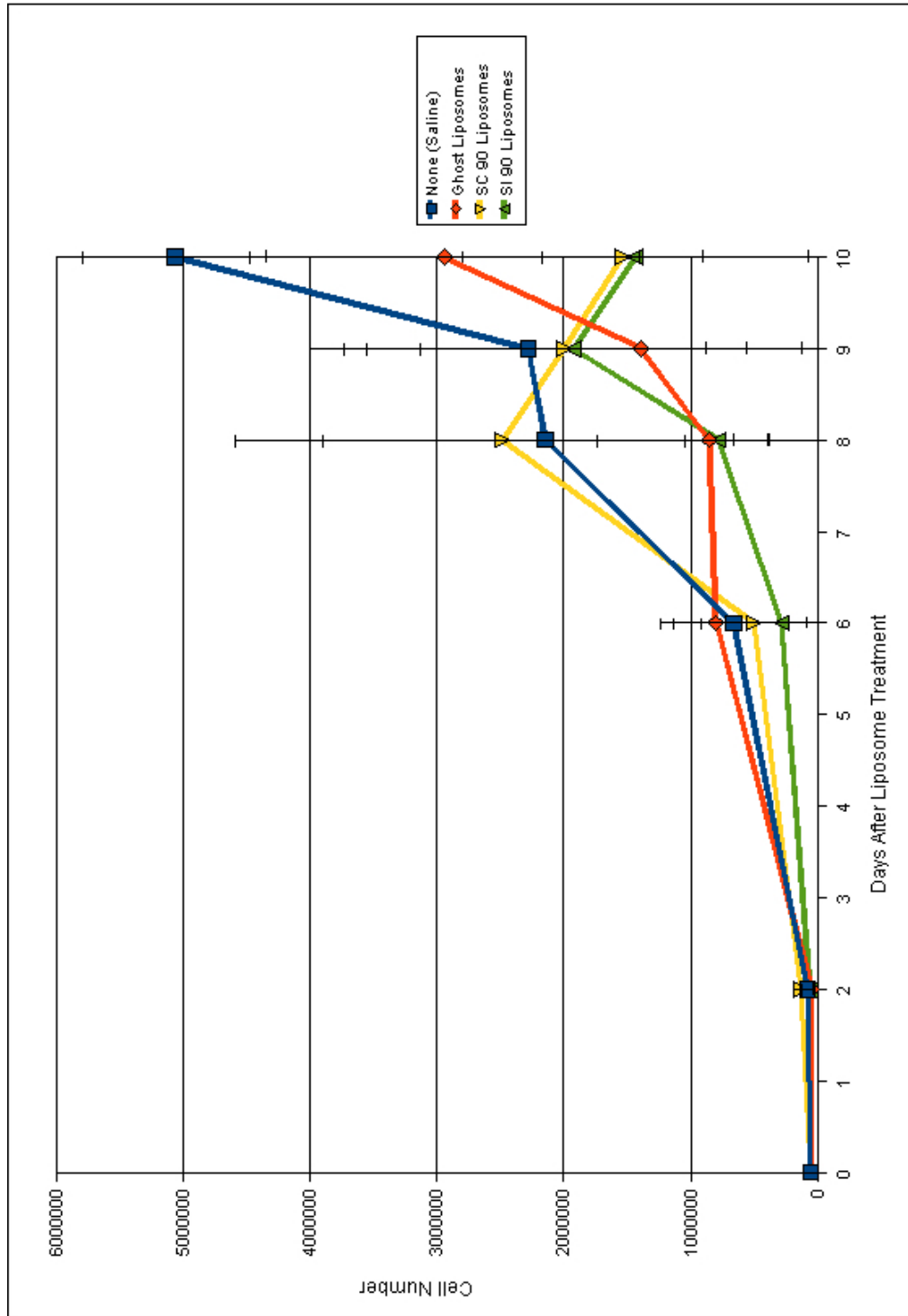


Figure 3-17: Graph of growth inhibition by liposome-mediated transfection of siRNA targeted against position 90 of the gastrin mRNA in BxPC-3-Luc cells. Each data point indicates cell numbers \pm 1 standard deviation.

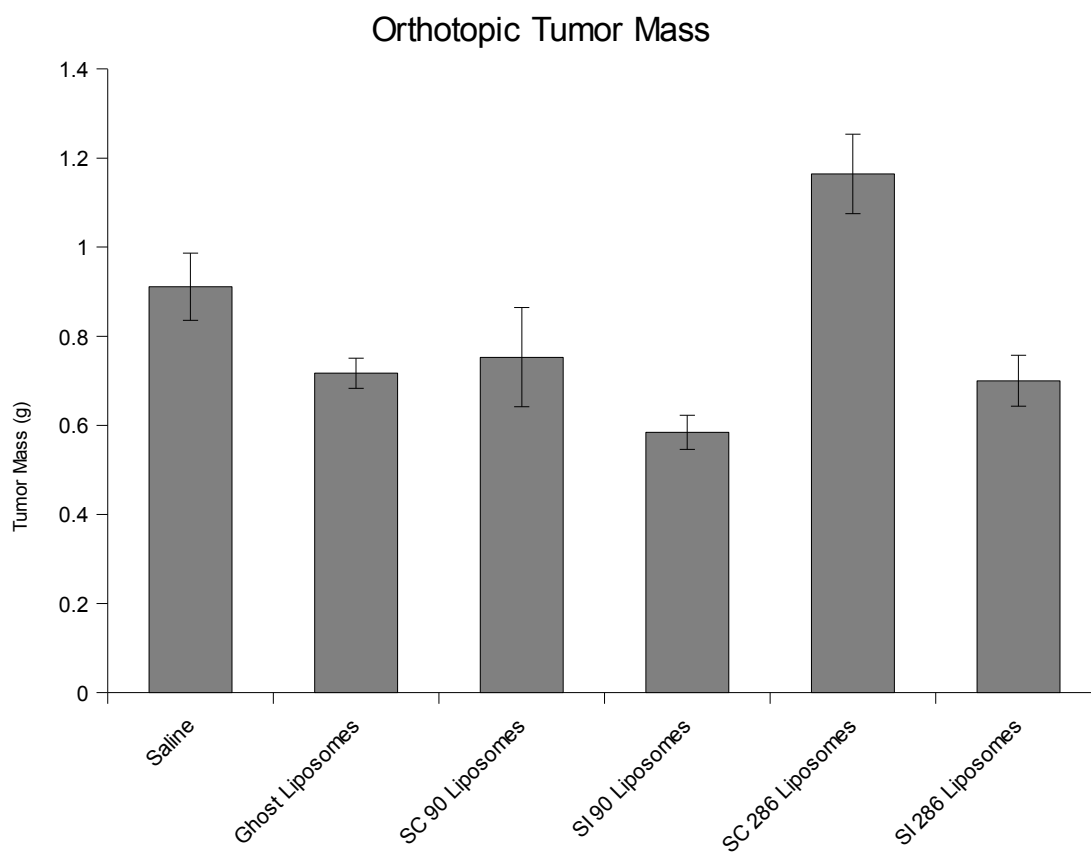


Figure 3-18: Tumor masses of liposome-treated orthotopic tumors in athymic nude mice. Graphs are tumor masses \pm 1 standard deviation.

BxPC-3-Luc Orthotopic Tumors

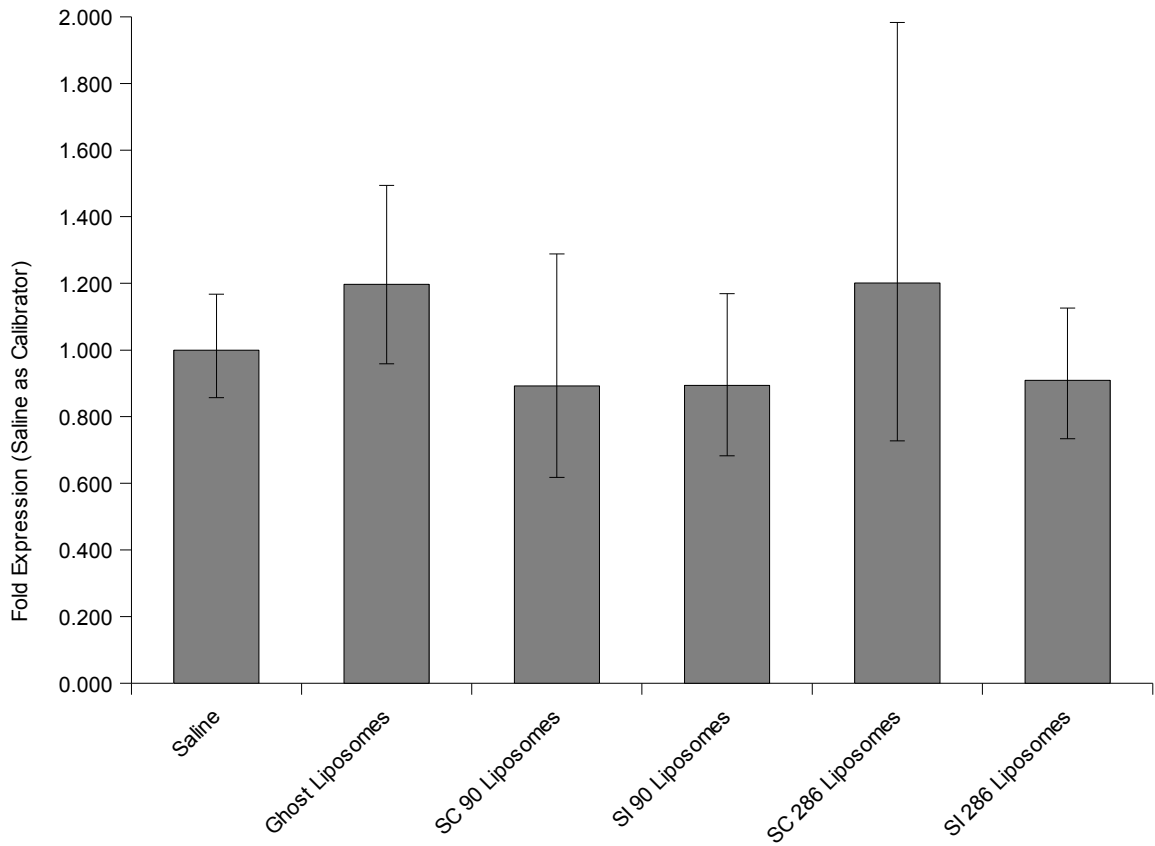


Figure 3-19: Real-time RT-PCR for gastrin of RNA isolated from liposome-treated orthotopic BxPC-3-Luc tumors in athymic nude mice. Graphs are in fold expression of gastrin \pm the maximum and minimum relative quantities

Table 3-1: Sedimentation of 100% pegylated liposome/siRNA mixtures prepared in sterile 0.9% saline.

siRNA Amount	Sedimentation
0X (Empty)	No
1X	No
2X	No
3X	No
4X	No
5X	No
6X	Yes
7X	Yes
8X	Yes
9X	Yes
10X	Yes

Table 3-2: Sedimentation of 75% pegylated liposome/siRNA mixtures prepared in 0.9% sterile saline and in dH₂O.

SiRNA Amount	Sedimentation in Saline-Prepared Liposomes	Sedimentation in dH ₂ O-Prepared Liposomes
0X (Empty)	No	No
1X	No	No
2X	No	No
3X	No	No
4X	Yes	No
5X	Yes	Yes
6X	Yes	Yes
7X	Yes	Yes
8X	Yes	Yes
9X	Yes	Yes
10X	Yes	Yes

Chapter 4

Discussion of Results

Pancreatic cancer continues to be one of the most quickly-progressing and lethal of all forms of cancer. It also remains one of the most difficult cancers to treat because of the advanced stage that it is often diagnosed at, along with its resistance to many chemotherapeutic agents (1, 3). The few treatment options that are available do little to improve survival time. The best hope for treatment is early detection and surgical removal of the cancer before it has reached an advanced stage or metastasized (3, 14). With Gemcitabine as the only realistic chemotherapeutic agent for pancreatic cancer (14), it is imperative to develop new targeted treatment strategies to inhibit pancreatic cancer growth and increase the chances of surgical removal of pancreatic tumors, which is the best current treatment option for pancreatic cancer (3). Targeted treatments can reduce the need for chemotherapeutic agents or enhance the ability of agents such as Gemcitabine, as was suggested by Watson and colleagues (50, 52, 57). Our laboratory's previous work with gastrin has established that gastrin is an important growth-stimulating factor for pancreatic cancer cells (77). Our laboratory has also revealed that antisense RNA and shRNA-mediated down-regulation of gastrin can inhibit the growth of pancreatic cancer cells *in vitro* and *in vivo* (Matters G, in press). Grabowska and colleagues have established that siRNAs targeted against gastrin can down-regulate gastrin mRNA in pancreatic cancer cells (19). These previous findings suggest that gastrin can be a potential therapeutic target for pancreatic cancer, and also that

developing an siRNA-based treatment system to down-regulate gastrin may improve upon results to what was obtained with shRNA and antisense RNA.

In order for siRNA to be a potential treatment strategy, an effective delivery method needed to be developed. Naked, unmodified RNA is not stable in serum (63, 64, 65), so a serum-stable carrier needs to be developed in order to efficiently deliver the siRNA to the proper cells. To that end, we have developed a nanoliposome-based delivery system that encapsulates and delivers anti-gastrin siRNA to pancreatic cancer cells. This system is based on a liposome delivery strategy developed by Tran and colleagues (76). This system has down-regulated gastrin mRNA in AsPC-1-Luc cells, down-regulated gastrin mRNA and gastrin peptide in BxPC-3-Luc cells, and inhibited the growth of BxPC-3-Luc cells *in vitro*. Our delivery system was also used *in vivo* in athymic nude mice against orthotopic BxPC-3-Luc tumors. The liposome treatments, given three times a week, were not toxic to the mice (data not shown). The results obtained in this series of experiments establish a trend in favor of down-regulation of gastrin mRNA by siRNA molecules targeted against positions 90 and 286 of the gastrin mRNA. However, this system did not obtain consistent statistical significance in terms of gastrin mRNA down-regulation and inhibition of tumor growth when compared to the saline control group. A more consistent down-regulation needs to be obtained before this system can be considered to be an effective treatment system. For these reasons, improvements to the liposome-mediated siRNA delivery system must be made before this system becomes a viable treatment strategy *in vivo*.

A possible future direction in this study that may potentially improve down-

regulation of gastrin mRNA and gastrin peptide could be the targeting of the liposomes specifically to pancreatic cancer cells. Liposome targeting has successfully been attempted by several groups to enhance the delivery of therapeutic agents or siRNA in different *in vitro* systems (82, 83, 84, 85, 95, 97). Specific to our study is the possibility to attach gastrin peptides to the liposomes, which would likely increase the number of liposomes that deliver siRNA to the pancreatic tumors, increasing transfection efficiency. This would also likely lower the binding of liposomes to cells other than pancreatic cancer cells. For example, Pastorino and colleagues have developed a targeted liposome designed to deliver doxorubicin to blood vessels and inhibit tumor growth. They accomplished liposome targeting by linking a peptide to a polyethylene glycol (PEG) group on the liposome via a maleimide linkage involving an amino-terminal cysteine residue added onto the peptide (82). In our study, the liposome formulations also contain PEG groups, so it may be possible to modify the method developed by Pastorino to generate gastrin-laden liposomes that would specifically target pancreatic cancer cells. Also to the favor of the development of gastrin-laden liposomes is a finding by Tarasova and colleagues that gastrin and the CCK2R are taken into the cell by endocytosis upon gastrin binding to the CCK2R in various gastric cancer cell lines such as the rat pancreatic cancer cell line AR42J. The CCK2R is then recycled back to the cell membrane (96). These results suggest that the CCK2R could be used as a target for drug delivery to deliver anti-gastrin siRNA to cells, although the Tarasova group suggests that drugs that bind to the CCK2R could be internalized and remain compartmentalized within the cells, unable to produce any effects on cell function. This is a concern that

may be important when developing gastrin-laden liposomes.

Another consideration related to optimized liposome uptake would be the amount of PEG groups present on the liposomes. An effective *in vivo* liposome treatment against pancreatic cancer needs to ensure high uptake in as many tumor cells as possible. Previous studies in our laboratory have shown that different pancreatic cancer cell lines have different liposome uptake rates, and that altering the PEG concentrations on liposomes impacts uptake rates in these cell lines. It is important to consider PEG concentration not only in terms of pancreatic cancer cell uptake in more cell lines than the ones used in this study, but also in terms of the effectiveness of the gastrin-laden liposomes, which require PEG groups for gastrin linkage.

Several issues arose in the *in vivo* study that will need to be resolved in order for this liposome-based strategy to become a potential treatment strategy for pancreatic cancer. In the study, a “ghost effect” occurred where the average mass of the tumors in mice treated with empty liposomes was similar to the average tumor mass in mice treated with anti-gastrin siRNA (Figure 3-18). It is believed that this could be a result of a charge difference between empty liposomes and liposomes complexed with siRNA, possibly being toxic to the cancer cells.

Another potential issue with the *in vivo* study deals with the route of administration of the liposome/siRNA mixtures. All injections were done via the lateral tail vein of each mouse three times a week for eight weeks. The number of injections led to scarring in many of the mice, making it difficult to successfully inject the mice at later points in the study. Also, five mice in the study died from reactions to the tail vein

injections, possibly from cardiac arrest. Finally, the liposome/siRNA mixtures did not always completely enter the tail vein when injected. The liquid would form a bolus at the injection site, resulting in fewer liposomes entering the circulation and lowering the therapeutic effect on the orthotopic tumors. Changing the injection route to either intramuscular or intraperitoneal may increase the amount of liposomes that reach the pancreatic tumors.

In conclusion, we have developed a liposome-mediated siRNA delivery system for anti-gastrin siRNA to be delivered to pancreatic cancer cells. This system is a novel treatment strategy that takes advantage of the fact that gastrin is a hormone that stimulates the growth of pancreatic cancer and is not produced in the pancreas at any other point except for during fetal development. This system is able to hold a finite amount of anti-gastrin siRNA. It can down-regulate gastrin mRNA in the AsPC-1-Luc and BxPC-3-Luc pancreatic cancer cell lines, and can also down-regulate the gastrin peptide in the BxPC-3-Luc cell line. This down-regulation of gastrin may also inhibit the growth of BxPC-3-Luc cells *in vitro*. This delivery system was not toxic to athymic nude mice, but it did not significantly down-regulate gastrin mRNA or inhibit the growth of orthotopic BxPC-3-Luc tumors in the mice. In order to make this trend toward down-regulation more statistically significant, additional work needs to be done to increase the transfection efficiency of the liposomes *in vitro* and *in vivo*. Modifications to the liposome-mediated delivery system, such as developing gastrin-laden liposomes, modifying the pegylation content of the liposomes, and determining the most effective injection route, may make this delivery system a stronger treatment strategy for

pancreatic cancer that may ultimately translate to humans.

BIBLIOGRAPHY

1. Jemal A, Siegel R, Ward E, Hao Y, Xu J, Murray T, and Thun M. Cancer statistics, 2008. *CA Cancer J Clin* 2008;58:71-96.
2. Koorstra J-B, Hustix S, Offerhaus G, and Maitra A. Pancreatic carcinogenesis. *Pancreatology* 2008;8:110-125.
3. Ghaneh P, Costello E, and Neoptolemos J. Biology and management of pancreatic cancer. *Gut* 2007;56:1134-1152.
4. Kern S, Hruban R, Hidalgo M, and Yeo C. An introduction to pancreatic adenocarcinoma genetics, pathology, and therapy. *Cancer Biol Ther* 2002;1(6):607-613.
5. Zheng W, McLaughlin J, Gridley G, Bjelke E, Schuman L, Silverman D, Wacholder S, Co-Chien H, Blot W, and Fraumeni J. A cohort study of smoking, alcohol consumption, and dietary factors for pancreatic cancer (United States). *Cancer Genes Control* 1993;4:477-482.
6. Hecht S. Cigarette smoking: cancer risks, carcinogens, and mechanisms. *Langenbecks Arch Surg* 2006;391:603-613.
7. Hruban R, Adsay N, Albores-Saavedra J, Compton C, Garrett E, Goodman S, Kern S, Klimstra D, Kloppel G, Longnecker D, Luttges J, and Offerhaus G. Pancreatic intraepithelial neoplasia: a new nomenclature and classification system for pancreatic duct lesions. *Am J Surg Path* 2001;25(5):579-586.
8. Hruban R, Goggins M, Parsons J, and Kern S. Progression model for pancreatic cancer. *Clin Cancer Res* 2000;6:2969-2972.

9. Takaori K. Current understanding of precursors to pancreatic cancer. *J Hepatobiliary Pancreat Surg* 2007;14:217-223.
10. Smit V, Boot A, Smits A, Fleuren G, Cornelisse C, and Bos J. KRAS codon 12 mutations occur very frequently in pancreatic adenocarcinomas. *Nucl Acids Res* 1988;16(16): 7773-7782.
11. Siveke J, Schmid R. Chromosomal instability in mouse metastatic pancreatic cancer-it's Kras and Tp53 after all. *Cancer Cell* 2005;405-407.
12. Bardeesy N, Aguirre A, Chu G, Cheng K-H, Lopez L, Hezel A, Feng B, Brennan C, Weissleder R, Mahmood U, Hanahan D, Redston M, Chin L, and DePinho R. Both p16^{Ink4A} and the p19^{ARF}-p53 pathway constrain progression of pancreatic adenocarcinoma in the mouse. *Proc Natl Acad Sci USA* 2006;103(15):5947-5952.
13. Hansel D, Kern S, and Hruban R. Molecular pathogenesis of pancreatic cancer. *Annu Rev Genomics Hum Genet* 2003;4:237-256.
14. Maitra A. and Hruban R. Pancreatic cancer. *Annu Rev Pathol Mech Dis* 2008;3:157-188.
15. Saif M. Pancreatic cancer: is this bleak landscape finally changing? *J Pancreas* 2007;8(4):365-373.
16. Hilbig A, Oettle H. Gemcitabine in the treatment of pancreatic cancer. *Exp Rev Anticancer Ther* 2008;8(4):511-523.
17. Bendell J, Goldberg R. Targeted agents in the treatment of pancreatic cancer: history and lessons learned. *Curr Opin Oncology* 2007;19:390-395.

18. Von Hoff D. What's new in the pancreatic cancer treatment pipeline? *Best Pract Res Clin Gastro* 2006;20(2):315-326.
19. Grabowska A, Hughes J, and Watson S. Use of interfering RNA to investigate the role of endogenous gastrin in the survival of gastrointestinal cancer cells. *Br J Cancer* 2007;96:464-473.
20. Grabowska A, Watson S. Role of gastrin peptides in carcinogenesis. *Cancer Lett* 2007;257:1-15.
21. Wiborg O, Berglund L, Boel E, Norris F, Norris K, Rehfeld J, Marcker K, and Vuust J. Structure of a human gastrin gene. *Proc Natl Acad Sci USA* 1984;81:1067-1069.
22. Dufresne M, Seva C, and Fourmy D. Cholecystokinin and gastrin receptors. *Physiol Rev* 2006;86:805-847.
23. Dockray G, Dimaline R, and Varro A. Gastrin: old hormone, new functions. *Pflugers Arch – Eur J Physiol* 2005;449:344-355.
24. Dockray G, Varro A, Dimaline R, and Wang T. The gastrins: their production and biological activities. *Annu Rev Physiol* 2001;63:119-139.
25. Miller L, Gao F. Structural basis of cholecystokinin receptor binding and regulation. *Pharm Thera* 2008;119:83-95.
26. Ferrand A, Wang T. Gastrin and cancer: A review. *Cancer Lett* 2006;238:15-29.
27. Rozengurt E, Walsh J. Gastrin, CCK, signaling, and cancer. *Annu Rev Physiol* 2001;63:49-76.

28. Arnould M, Tassa A, Ferrand A, Archer E, Esteve J-P, Penalba V, Portolan G, Escherich A, Moroder L, Fourmy D, Seva C, and Dufresne M. The G-protein-coupled CCK2 receptor associates with phospholipase $C\gamma 1$. *FEBS Lett* 2004;568:89-93.
29. Hollestelle M, Timmermann P, Meloen R, and Hoppener J. Characterization of gastrin-cholecystokinin 2 receptor interaction in relation to c-fos induction. *Endoc Relat Cancer* 2008;15(1):301-309.
30. Todisco A, Takeuchi Y, Seva C, Dickinson C, and Yamada T. Gastrin and glycine-extended progastrin processing intermediates induce different programs of early gene activation. *J Biol Chem* 1995;270:47:28337-28341.
31. Ferrand A, Kowalski-Chauvel A, Bertrand C, Escrieut C, Mathieu A, Portolan G, Pradayrol L, Fourmy D, Dufresne M, and Seva C. A novel mechanism for JAK2 activation by a G-protein-coupled receptor, the CCK2R. *J Biol Chem* 2005;280(11):10710-10715.
32. Schubert M, Peura D. Control of gastric acid secretion in health and disease. *Gastroenterology* 2008;134:1842-1860.
33. Watson S, Grabowska A, El-Zaatari M, and Takhar A. Gastrin – active participant or bystander in gastric carcinogenesis? *Nat Rev Cancer* 2006;6:936-946.
34. Nagata A, Ito M, Iwata N, Kuno J, Takano H, Minowa O, Chihara K, Matsui T, and Noda T. G protein-coupled cholecystokinin-B/gastrin receptors are responsible for physiological cell growth of the stomach mucoas in vivo. *Proc Natl Acad Sci USA* 1996;93:11825-11830.

35. Iwase K, Evers B, Hellmich M, Guo Y-S, Higashide S, Kim H, and Townsend C. Regulation of growth of human gastric cancer by gastrin and glycine-extended progastrin. *Gastroenterology* 1997;113:782-790.
36. Morriset J. Hormonal control of pancreatic growth during fetal, neonatal and adult life. *Adv Med Sci* 2008;53(2):99-118.
37. Morriset J, Laine J, Biernat M, and Julien S. What are the pancreatic target cells for gastrin and its CCK_B receptor? Is this a couple for cancerous cells? *Med Sci Monit* 2004;10(10):RA242-246.
38. Guo-Y-S, Townsend C. Roles of gastrointestinal hormones in pancreatic cancer. *J Hepatobiliary Pancreat Surg* 2000;7:276-285.
39. Goetze J, Nielsen F, Burcharth F, and Rehfeld J. Closing the gastrin loop in pancreatic carcinoma: Coexpression of gastrin and its receptor in solid human pancreatic adenocarcinoma. *Cancer* 2000;88(11):2487-2493.
40. Caplin M, Savage K, Khan K, Brett B, Rode J, Varro A, and Dhillon A. Expression and processing of gastrin in pancreatic adenocarcinoma. *Br J Surg* 2000;87:1035-1040.
41. Clarke P, Dickson J, Harris J, Grabowska A, and Watson S. Gastrin enhances the angiogenic potential of endothelial cells via modulation of heparin-binding epidermal-like growth factor. *Cancer Res* 2006;66(7):3504-3512.
42. Smith J, Shih A, Wotring M, McLaughlin P, and Zagon I. Characterization of CCK-B/gastrin-like receptors in human gastric carcinoma. *Int J Onc* 1998;12:411-419.

43. Smith J, Shih A, Wu Y, McLaughlin P, and Zagon I. Gastrin regulates growth of human pancreatic cancer in a tonic and autocrine fashion. *Am J Physiol Reg Integr Comp Physiol* 1996;270:1078-1084.
44. Smith J., Fantaskey A, Liu G, and Zagon I. Identification of gastrin as a growth peptide in human pancreatic cancer. *Am J Physiol Reg Integr Comp Physiol* 1995;268:135-141.
45. Smith J, Liu G, Soundararajan V, McLaughlin P, and Zagon I. Identification and characterization of CCK-B/gastrin receptors in human pancreatic cancer cell lines. *Am J Physiol Reg Integr Comp Physiol* 1994;266:277-283.
46. Smith J, Stanley W, Verderame M, and Zagon I. The functional significance of the cholecystokinin-C (CCK-C) receptor in human pancreatic cancer. *Pancreas* 2004;29(4):271-7.
47. Ding W-Q, Kuntz S, and Miller L. A misspliced form of the cholecystokinin-B/gastrin receptor in pancreatic carcinoma: Role of reduced cellular U2AF35 and a suboptimal 3'-splicing site leading to retention of the fourth intron. *Cancer Res* 2002;62:947-952.
48. Gales C, Sanchez D, Poirot M, Pyronnet S, Buscail L, Cussac D, Pradayrol L, Fourmy D, and Silvente-Poirot S. High tumorigenic potential of a constitutively active mutant of the cholecystokinin 2 receptor. *Oncogene* 2003;22(38):6081-6088.
49. Hellmich M, Rui X-L, Hellmich H, Fleming R, Evers B, and Townsend C. Human colorectal cancers express a constitutively active cholecystokinin-

- B/gastrin receptor that stimulates cells growth. *J Biol Chem* 2000;275(41):32122-32128.
50. Harris J, Gilliam A, McKenzie A, Evans S, Grabowska A, Clarke P, McWilliams D, and Watson S. The biological and therapeutic importance of gastrin gene expression in pancreatic adenocarcinomas. *Cancer Res* 2004;64:5624-5631.
51. Berna M, Tapia J, Sancho V, and Jensen R. Progress in developing cholecystokinin (CCK)/gastrin receptor ligands that have therapeutic potential. *Curr Opin Pharm* 2007;7:583-592.
52. Watson S, Michaeli D, Grimes S, Morris T, Robinson G, Varro A, Justin T, and Hardcastle J. Gastrimmune raises antibodies that neutralize amidated and glycine-extended gastrin-17 and inhibit the growth of colon cancer. *Cancer Res* 1996;56:880-885.
53. Chau I, Cunningham D, Russell C, Norman A, Kurzawinski T, Harper P, Harrison P, Middleton G, Daniels F, Hickish T, Prendeville J, Ross P, Theis B, Hull R, Walker M, Shankley N, Kalindjian B, Murray G, Gillbanks A, and Black J. Gastrazole (JB95008), a novel CCK2/gastrin receptor antagonist, in the treatment of advanced pancreatic cancer: results from two randomised controlled trials. *Br J Cancer* 2006;94:1107-1115.
54. Savage K, Waller H, Stubbs M, Khan K, Watson S, Clarke P, Grimes S, Michaeli D, Dhillon A, and Caplin M. Targeting of cholecystokinin B/gastrin receptor in colonic, pancreatic and hepatocellular carcinoma cell lines. *Int J Oncology* 2006;29:1429-1435.

55. Barderas R, Shochat S, Timmermann P, Hollestelle M, Martinez-Torrecuadrada J, Hoppener J, Altschuh D, Meloen R, and Casal J. Designing antibodies for the inhibition of gastrin activity in tumoral cell lines. *Int J Cancer* 2008;122:2351-2359.
56. Sosabowski J, Lee M, Dekker B, Simmons B, Singh S, Beresford H, Hagan S, McKenzie A, Mather S, and Watson S. Formulation development and manufacturing of a gastrin/CCK-2 receptor targeting peptide as an intermediate drug product for a clinical imaging study. *Eur J Pharm Sci* 2007;31:102-111.
57. Fire A, Xu S, Montgomery M, Kostas S, Driver S, and Mello C. Potent and specific genetic interference by double-stranded RNA in *Caenorhabditis elegans*. *Nature* 1998;391:806-811.
58. Dykxhoorn D, Lieberman J. Running interference: prospects and obstacles to using small interfering RNAs as small molecule drugs. *Annu Rev Biomed Eng* 2006;8:377-402.
59. Gewirtz A. On future's doorstep: RNA interference and the pharmacopeia of tomorrow. *J Clin Invest* 2007;117(12):3612-3614.
60. Iorns E, Lord C, Turner N, and Ashworth A. Utilizing RNA interference to enhance cancer drug discovery. *Nat Rev Drug Disc* 2007;6:556-568.
61. Corey D. Chemical modification: the key to clinical application of RNA interference? *J Clin Invest* 2007;117(12):3615-3622.

62. Kumar L, Clarke A. Gene manipulation through the use of small interfering RNA (siRNA): from in vitro to in vivo applications. *Adv Drug Del Rev* 2007;59:87-100.
63. Kawakami S, Hashida M. Targeted delivery systems of small interfering RNA by systemic administration. *Drug Met Pharmacokinetics* 2007;22(3):142-151.
64. Pirollo K, Chang E. Targeted delivery of small interfering RNA: approaching effective cancer therapies. *Cancer Res* 2008;68(5):1247-1250.
65. Behlke M. Progress toward in vivo use of siRNAs. *Mol Ther* 2006;13:644-670.
66. Jackson A, Bartz S, Schelter J, Kobayashi S, Burchard J, Mao M, Li B, Cavet G, and Linsley P. Expression profiling reveals off-target gene regulation by RNAi. *Nat Biotech* 2003;21(6):635-637.
67. Grimm D, Streetz K, Jopling C, Storm T, Pandey K, Davis C, Marion P, Salazar F, and Kay M. Fatality in mice due to oversaturation of cellular microRNA/short hairpin RNA pathways. *Nature* 2006;441:537-541.
68. Xie F, Woodle M, and Lu P. Harnessing in vivo siRNA delivery for drug discovery and therapeutic development. *Drug Disc Today* 2006;11(1/2):67-73.
69. Akhtar S, Benter I. Nonviral delivery of synthetic siRNAs in vivo. *J Clin Invest* 2007;117(12):3623-3632.
70. Zimmermann T, Lee A, Akinc A, Bramlage B, Bumcrot D, Fedoruk M, Harborth J, Heyes J, Jeffs L, John M, Judge A, Lam K, McClintock K, Nechev L, Palmer L, Racie T, Rohl I, Seiffert S, Shanmugam S, Sood V, Soutschek J, Toudjarska I, Wheat A, Yaworski E, Zedalis W, Koteliansky V, Manoharan M, Vornlocher H-P,

- and MacLachlan I. RNAi-mediated gene silencing in non-human primates. *Nature* 2006;441:111-114.
71. Pellish R, Nasir A, Ramratnam B, and Moss S. Review article: RNA interference – potential therapeutic applications for the gastroenterologist. *Aliment Pharm Ther* 2008;27:715-723.
72. Wang J, Shi Y, Yi J, Ye S, Wang L, Xu Y, He M, and Kong X. Suppression of growth of pancreatic cancer cell and expression of vascular endothelial growth factor by gene silencing with RNA interference. *J Dig Dis* 2008;9:228-237.
73. Smith J, Verderame M, and Zagon I. Antisense oligonucleotides to gastrin inhibit growth of human pancreatic cancer. *Cancer Lett* 1999;135:107-112.
74. Fenske D, Chonin A, and Cullis P. Liposomal nanomedicines: An emerging field. *Toxicological Path* 2008;36:21-29.
75. Fenske D, Cullis P. Entrapment of small molecules and nucleic acid-based drugs in liposomes. *Methods Enzymology* 2005;391:7-39.
76. Tran M, Gowda R, Sharma A, Park E-J, Adair J, Kester M, Smith N, and Robertson G. Targeting V600EB-Raf and Akt3 using nanoliposomal-small interfering RNA inhibits cutaneous melanocytic lesion development. *Cancer Res* 2008;68(18):7638-7649.
77. Smith J, Verderame M, Ballard E, and Zagon I. Functional significance of gastrin gene expression in human cancer cells. *Reg Peptides* 2004;117:167-173.
78. Blume G, Cevc G. Liposomes for the sustained drug release in vivo. *Biochim Biophys Acta* 1990;1029:91-97.

79. Almofti M, Harashima H, Shinohara Y, Almofti A, Baba Y, and Kiwada H. Cationic liposome-mediated gene delivery: Biophysical study and mechanism of internalization. *Arch Biochem Biophys* 2003;410:246-253.
80. Devalapally H, Chakliam A, and Amiji M. Role of nanotechnology in pharmaceutical development. *J Pharm Sci* 2007;96(10):2547-2565.
81. Akhtar S, Benter I. Toxicogenomics of non-viral drug delivery systems for RNAi: Potential impact on siRNA-mediated gene silencing activity and specificity. *Adv Drug Del Rev* 2007;59:164-182.
82. Pastorino F, Brignole C, Marimpietri D, Cilli M, Gambini C, Ribatti D, Longhi R, Allen T, Corti A, and Ponzoni M. Vascular damage and anti-angiogenic effects of tumor vessel-targeted liposomal chemotherapy. *Cancer Res* 2003;63:7400-7409.
83. Reddy J, Abburi C, Hofland H, Howard S, Vlahov I, Wils P, and Leamon C. Folate-targeted, cationic liposome-mediated gene transfer into disseminated peritoneal tumors. *Gene Ther* 2002;9:1542-1550.
84. Lee R, Huang L. Folate-targeted, anionic liposome-entrapped polylysine-condensed DNA for tumor cell-specific gene transfer. *J Biol Chem* 1996;271(14):8481-8487.
85. Holig P, Bach M, Volkel T, Nahde T, Hoffmann S, Muller R, and Kontermann R. Novel RDG lipopeptides for the targeting of liposomes to integrin-expressing endothelial and melanoma cells. *Prot Eng Design Selection* 2004;17(5):433-441.
86. Szoka F. The art of assembly. *Science* 2008;319:578-579.

87. Lv H, Zhang S, Wang B, Cui S, and Yan J. Toxicity of cationic lipids and cationic polymers in gene delivery. *J Controlled Release* 2006;114:100-109.
88. Allen T, Hansen C, and Rutledge J. Liposomes with prolonged circulation times: factors affecting uptake by reticuloendothelial and other tissues. *Biochim Biophys Acta* 1989;981:27-35.
89. Gabizon A, Catane R, Uziely B, Kaufman B, Safra T, Cohen R, Martin F, Huang A, and Barenholz Y. Prolonged circulation time and enhanced accumulation in malignant exudates of doxorubicin encapsulated in polyethylene-glycol coated liposomes. *Cancer Res* 1994;54:987-992.
90. Almofti M, Harashima H, Shinohara Y, Almofti A, Li W, and Kiwada H. Lipoplex size determines lipofection efficiency with or without serum. *Molec Membrane Biol* 2003;20(1):35-43.
91. Li S-D, Huang L. Gene therapy progress and prospects: non-viral gene therapy by systemic delivery. *Gene Ther* 2006;13:1313-1319.
92. Heidel J, Yu Z, Liu J, Rele S, Liang Y, Zeidan R, Kornbrust D, and Davis M. Administration in non-human primates of escalating intravenous doses of targeted nanoparticles containing ribonucleotide reductase subunit M2 siRNA. *Proc Natl Acad Sci USA* 2007;104(14):5715-5721.
93. Sipos B, Moser S, Kalthoff H, Torok V, Lohr M, and Kloppel G. A comprehensive characterization of pancreatic ductal carcinoma cell lines: towards the establishment of an in vitro research platform. *Virchows Arch* 2003;442:444-452.

94. Mandair K, Towner P, Stanford I, Morris J, Harper E, Benjamin I, and Tavares I. Cholecystokinin receptors in human pancreatic cancer cell lines. *Eur J Cancer* 1998;34(9):1455-1459.
95. Pirollo K, Rait A, Zhou Q, Hwang S, Dagata J, Zon G, Hogrefe R, Palchik G, and Chang E. Materializing the potential of small interfering RNA via a tumor-targeting nanodelivery system. *Cancer Res* 2007;67(7):2938-2943.
96. Tarasova N, Wank S, Hudson E, Romanov V, Czerwinski G, Resau J, and Michejda C. Endocytosis of gastrin in cancer cells expressing gastrin/CCK-B receptor. *Cell Tissue Res* 1997;287:325-333.
97. Peer D, Park E, Morishita Y, Carman C, and Shimaoka M. Systemic leukocyte-directed siRNA delivery revealing cyclin D1 as an anti-inflammatory target. *Science* 2008;319:627-630.